REPORT No. 573

AERODYNAMIC CHARACTERISTICS OF N. A. C. A. 23012 AND 23021 AIRFOILS WITH 20-PERCENT-CHORD EXTERNAL-AIRFOIL FLAPS OF N. A. C. A. 23012 SECTION

By Robert C. Platt and Ira H. Abbott

SUMMARY

The results of an investigation of the general aerodynamic characteristics of the N. A. C. A. 23012 and 23021 airfoils, each equipped with a 0.20c external-airfoil flap of N. A. C. A. 23012 section, are presented. The tests were made in the N. A. C. A. 7- by 10-foot and variable-density wind tunnels and covered a range of Reynolds Numbers that included values corresponding to those for landing conditions of a wide range of airplanes. Besides a determination of the variation of lift and drag characteristics with position of the flap relative to the main airfoil, complete aerodynamic characteristics of the airfoil-flap combination with a flap hinge axis selected to give small hinge moments were measured in the two tunnels. Some measurements of air loads on the flap itself in the presence of the wing were made in the 7- by 10-foot wind tunnel.

From the data obtained, the external-airfoil flap in combination with an airfoil appears to be one of the most generally satisfactory high-lift devices investigated to date. The combination tested offers a relatively high value of maximum lift coefficient with low profile drag in the high-lift range. At low lift coefficients it gives very nearly as low values of profile drag as a good plain airfoil of comparable thickness. Structural and stability problems associated with the large negative pitching moments occurring at high lift coefficients may be slightly greater than in the case of ordinary and split flaps.

INTRODUCTION

Consideration of the external-airfoil flap as a high-lift device indicates that it may be generally applied to improve airplane performance. Previous investigations of this device (see reference 1) have shown that it is capable of developing high lift coefficients and that it gives lower drag at these high lift coefficients than ordinary or split flaps. Thus it may be more favorable to such items of performance as take-off and ceiling. In addition, it can be balanced to have very low operating moments throughout its range of deflection and, if large adverse yawing moments are acceptable, it may be used to obtain lateral control while still extending over the full wing span as a high-lift device.

Good aerodynamic characteristics have been obtained with an external-airfoil flap of Clark Y section (reference 1), especially when used in connection with a main airfoil of N. A. C. A. 23012 section. Consideration of known scale effect and drag characteristics of the Clark Y and N. A. C. A. 23012 airfoils indicated that substituting the N. A. C. A. 23012 section for the Clark Y section of the flap might improve the speed-range index of the combination. In addition, the small

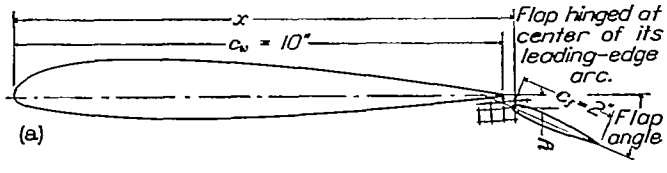

(a) Survey of flap positions.

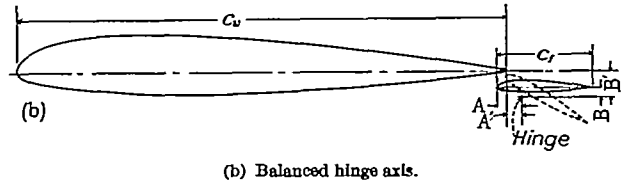

(b) Balanced hinge axis.

	Axis 1	Axis 2
A	0.250c_f	0.240c_f
B	.100c_f	.100c_f
A'	.032c_w	.030c_w
B'	.054c_w	.054c_w

FIGURE 1.—Flap-setting details. The N. A. C. A. 23012 airfoil with 0.20c_w N. A. C. A. 23012 external-airfoil flap.

center-of-pressure travel of the N. A. C. A. 23012 airfoil indicated the possibility of hinging it as a flap in such a manner that operating moments lower than those of the Clark Y flap might be obtained.

A preliminary investigation of the N. A. C. A. 23012 section used for both the main airfoil and the flap was made in the 7- by 10-foot wind tunnel to determine the variation of lift and drag characteristics with position of the flap relative to the main airfoil. A hinge-axis location intended to give low operating moments and good aerodynamic characteristics was then selected and final force tests were made with the flap hinged at this position and set at various angles.

The tests in the 7- by 10-foot wind tunnel were concluded with a determination of the air loads and the hinge moments on the flap.

A series of tests with the flap set at a few selected angles was made in the variable-density tunnel to determine the full-scale characteristics of the airfoil-flap combination developed in the 7- by 10-foot wind tunnel. Tests were then made of the N. A. C. A. 23021 airfoil with the N. A. C. A. 23012 flap, using the same hinge-axis location as with the N. A. C. A. 23012 airfoil. Although no tests of the combination with the N. A. C. A. 23021 airfoil were made in the 7- by 10-foot tunnel, analysis of the data of reference 1 indicated that the same flap hinge axis was optimum for either airfoil. The variable-density-tunnel tests covered a range of Reynolds Numbers representative of the landing conditions of most modern airplanes.

number of flap angles were investigated to determine the values of $C_{L_{max}}$ and $C_{D_{min}}$ obtainable at each flap position. In these tests the flap was hinged at the center of its leading-edge arc.

On the basis of results obtained from the foregoing tests, a new hinge axis giving reduced flap hinge moments and optimum aerodynamic characteristics at the various flap-angle settings was selected. The model with the flap hinged about this point, designated axis 1 in figure 1 (b), was used in a series of final force tests to determine the lift, drag, and pitching-moment characteristics of the airfoil-flap combination at the various flap-angle settings. The tests were conducted in accordance with standard force-test procedure in the 7- by 10-foot wind tunnel at a dynamic pressure of 16.37 pounds per square foot, corresponding to a speed of 80 miles per hour in standard air. The average

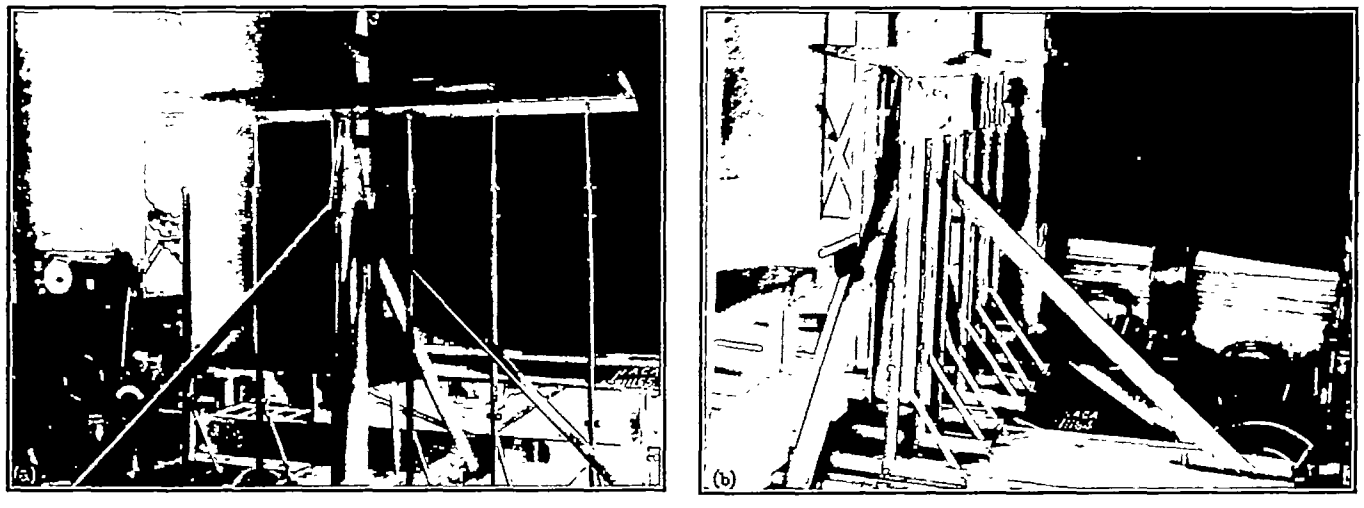

FIGURE 2.—Model arranged for flap-load tests in the 7- by 10-foot wind tunnel. The airfoil mounted on the balance; the flap separately supported.

APPARATUS, MODELS, AND TESTS

The tests were made during the summer of 1935 in the N. A. C. A. 7- by 10-foot and variable-density wind tunnels. Descriptions of the tunnels and the standard test procedures appear in references 2 and 3.

The model tested in the 7- by 10-foot wind tunnel was a rectangular airfoil of laminated mahogany having a span of 60 inches and a chord of 10 inches. The flap was a duralumin airfoil with a span of 60 inches and a chord of 2 inches. Fittings attached near the trailing edge of the airfoil supported the flap in any desired position relative to the airfoil. The N. A. C. A. 23012 airfoil model was the one used for the tests described in reference 1; likewise, the method of supporting the flaps, the program of testing, and the method of analyzing and presenting results were similar to those of reference 1. Figures 1, 2 and 3 are sketches and photographs of the models.

Tests in the 7- by 10-foot wind tunnel were first made to determine the variation of $C_{L_{max}}$ and $C_{D_{min}}$ of the airfoil-flap combination with the flap hinge located at each of the positions shown in figure 1 (a); a sufficient test Reynolds Number based on the 12-inch chord (wing chord+flap chord) of the model was approximately 730,000.

The variation with flap angle of flap hinge moment about axis 1 at a series of angles of attack was determined by measuring the twist of a calibrated rod attached to one end of the flap, which for this test was hinged freely on its supports. For reasons that will appear later, additional hinge-moment measurements about an axis slightly ahead of axis 1, designated axis 2 in figure 1 (b), were also made. Air loads on the flap itself were determined by supporting the flap separately in the correct position with respect to the main airfoil and measuring forces on the main airfoil alone. The flap loads were then readily computed by deducting the loads measured on the airfoil alone with the flap in the correct position from the forces measured on the combination in the previous force tests. Figure 2 shows the model arranged for flap-load measurements in the 7- by 10-foot wind tunnel. Similar measurements of flap loads and hinge moments on split flaps and Fowler flaps are described in references 4 and 5.

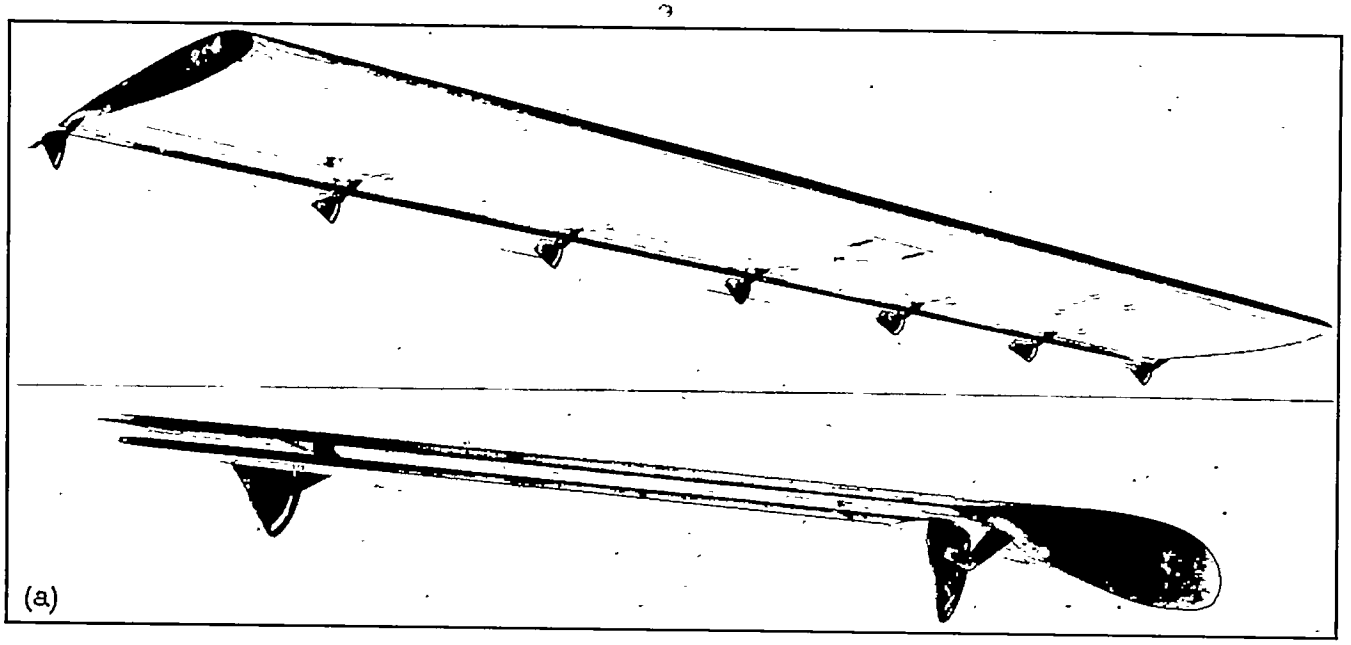

(a) Model used in the 7- by 10-foot wind tunnel.

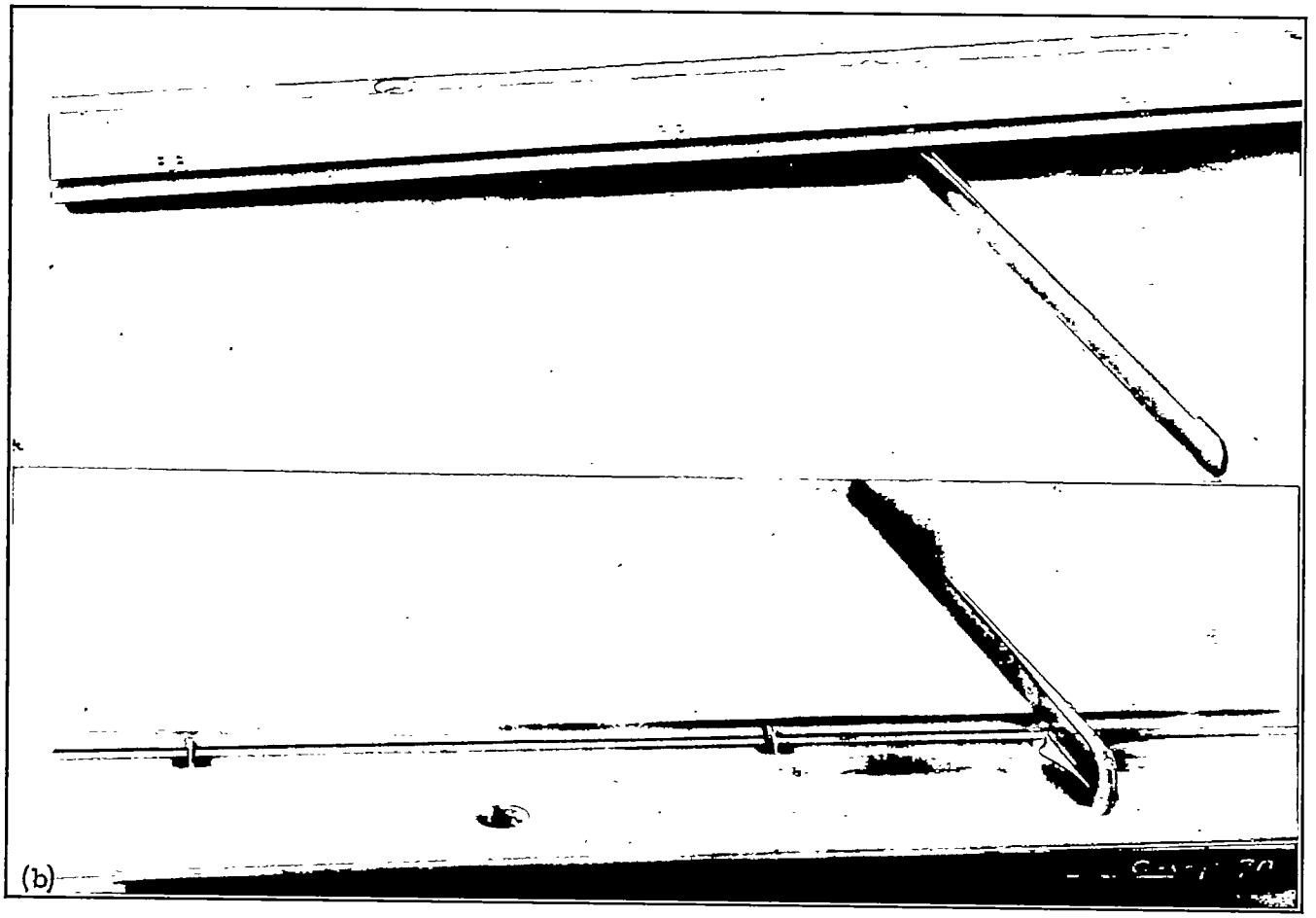

(b) Model used in the variable-density wind tunnel.

FIGURE 3.—The N. A. C. A. 23012 airfoil with 0.20c N. A. C. A. 23012 external-airfoil flap.

The models tested in the variable-density tunnel consisted of two duralumin airfoils of N. A. C. A. 23012 and N. A. C. A. 23021 sections using N. A. C. A. 23012 flaps made of stainless steel. The span of the models was 30 inches and the sum of the wing and flap chords, 5 inches. Small hinge brackets (fig. 3) were used to attach the flap to the main airfoils. Standard force tests were made at a Reynolds Number of about 3,000,000 (effective Reynolds Number about 8,000,000) of the combination using the N. A. C. A. 23012 section for the main airfoil with flap angles of −3°, 20°, 30°, and 40°. Similar tests with flap angles of −3° and 30° were made of the combination using the N. A. C. A. 23021 section for the main airfoil. Both combinations were tested inverted with the flap set at −3° (angle for minimum drag) to extend the characteristics through the negative-lift range. Maximum lift coefficients were also obtained for both combinations at lower values of the Reynolds Number.

PRECISION

The precision of force and load tests in the 7- by 10-foot wind tunnel is completely discussed in references 1, 4, and 5. A discussion of precision of force tests in the variable-density tunnel appears in references 3, 6, and 7. It is believed that the present test results may be considered free from any serious consistent errors and that they may be applied with normal engineering accuracy to free-flight conditions at the stated values of effective Reynolds Number.

RESULTS AND DISCUSSION

Form of presentation of results.—All test results have been reduced to standard nondimensional coefficient form based on total wing areas (sum of areas of airfoil and flap) and on total chord c (sum of chords of airfoil and flap), except the flap-load coefficients, which are based on the dimensions of the flap itself. The special coefficients used are defined as follows:

Subscript w refers to the main airfoil.

Subscript f refers to the flap.

$$C_{H_f}=\frac{\text{flap hinge moment}}{q(S_w+S_f)(c_w+c_f)}$$

$$C_{N_f}=\frac{\text{force on flap normal to flap chord}}{qS_f}$$

$$C_{c_f}=\frac{\text{force on flap parallel to flap chord}}{qS_f}$$

δ_f, angle between wing and flap chord lines, degrees.

$C_{m_{(a.c.)_0}}$, pitching-moment coefficient computed about the aerodynamic center determined for the airfoil-flap combination with the flap set at the minimum-drag angle.

Standard corrections for the effects of jet-boundary and static-pressure gradient in the 7- by 10-foot wind tunnel were applied to the test results. Although the nominal aspect ratio of the model having a span of 60 inches and a total chord of 12 inches was 5, the results have been corrected and are presented for aspect ratios of 6 and infinity. Infinite aspect ratio data are further corrected to an effective Reynolds Number to allow for the effects of air-stream turbulence, as explained in references 7 and 8.

The data obtained in the variable-density tunnel have been corrected in the usual manner (references 3, 9, and 10). The results are presented for an aspect ratio of 6 and as section data. The section characteristics, which have been corrected to the effective Reynolds Number and for the effect of rectangular tips (references 9 and 10), are distinguished from the wing characteristics by the use of lower-case letters, thus:

$$c_l, c_{d_0}, c_{m_{a.c.}}$$

Drag data obtained in both tunnels have been corrected by deducting the drag of the flap supports, estimated from tests with dummy supports. This correction was very small, varying in magnitude from 0 to 0.0005 at small and moderate values of the lift coefficient.

Determination of optimum flap hinge axis.—Results of the first series of tests in the 7- by 10-foot wind tunnel are given in figure 4. Contours showing the variation of $C_{L_{max}}$ with flap position at various flap angles appear in the figure, as well as contours of $C_{D_{min}}$ with the flap angle varying from −2° to −4°.

A balanced hinge axis for the flap was selected by investigating the characteristics of the wing-flap combination with the hinge axis near the 0.25 c_f point on the flap, where the flap hinge moments should be reduced to very small values. A profile of the flap drawn on transparent paper was laid on the various contour sheets and rotated about each of a series of hinge axes near the 0.25 c_f point on the flap and in various positions relative to the main airfoil; this procedure permitted the approximate determination of the values of $C_{L_{max}}$ and $C_{D_{min}}$ obtainable with the various axis locations. Hinge axis 1 (fig. 1 (b)) was finally selected as giving the best compromise between the requirements of low hinge moment, high $C_{L_{max}}$, and low $C_{D_{min}}$. The flap angles for $C_{L_{max}}$ and $C_{D_{min}}$ were 30° and −3°, respectively, and the loss of lift and drag characteristics incurred by hinging the flap at this axis was within the limits of accuracy of the tests in both cases.

Aerodynamic characteristics of selected airfoil combination.—Standard aerodynamic characteristics of the selected arrangement, as determined in the 7- by 10-foot wind tunnel, with the flap set at angles of −10°, −3°, 0°, 5°, 10°, 20°, 30°, and 40° are shown in figures 5 to 12, respectively. Similar data for the plain N. A. C. A. 23012 airfoil used in the tests are shown in figure 13.

It should be noted that the optimum flap angle for cruising and high-speed flight is not necessarily −3° but may vary somewhat with the lift coefficients corresponding to these speeds. The optimum angle for each design should probably be determined by flight test on account of possible variations resulting from such factors as the effect of attitude on fuselage and interference drag, the effect of pitching moment on tail drag, scale effect, and the variation with lift coefficient previously mentioned.

The results presented for the erect and inverted tests (figs. 14, 15, 19, and 20, and table I) overlap to some extent near zero lift and are not in strict agreement; the pitching-moment coefficients about the aerodynamic center, the positions of the aerodynamic center, and the values given in table I for the lift-curve slope, and for the angle of zero lift (indicated by the lift-curve slope) as obtained from the erect and inverted tests differ somewhat. These apparent discrepancies in table I arise from the fact that the

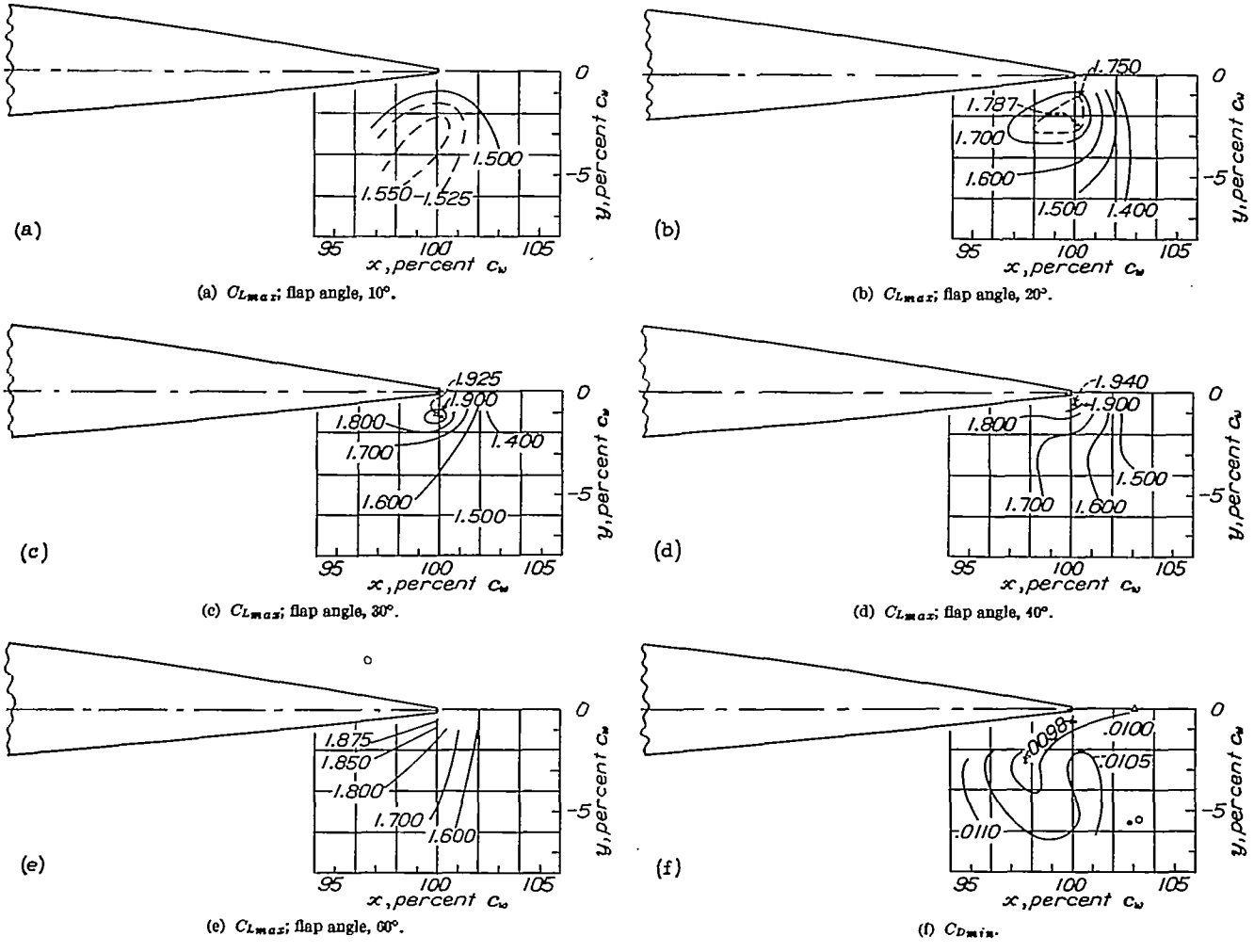

(a) $C_{L_{max}}$; flap angle, 10°.
(b) $C_{L_{max}}$; flap angle, 20°.
(c) $C_{L_{max}}$; flap angle, 30°.
(d) $C_{L_{max}}$; flap angle, 40°.
(e) $C_{L_{max}}$; flap angle, 60°.
(f) $C_{D_{min}}$.

FIGURE 4.—Contours showing variation of $C_{L_{max}}$ and $C_{D_{min}}$ with flap position and angle. The N. A. C. A. 23012 airfoil with 0.20c_w N. A. C. A. 23012 external-airfoil flap. Plain wing: $C_{L_{max}}$, 1.150; $C_{D_{min}}$, 0.0103.

Standard large-scale aerodynamic characteristics of the N. A. C. A. 23012 airfoil with the N. A. C. A. 23012 external-airfoil flap hinged at axis 2 (fig. 1(b)) at angles of −3° (upright and inverted), 20°, 30°, and 40° as obtained in the variable-density tunnel are shown in figures 14 to 18. Similar data for the N. A. C. A. 23021 airfoil in combination with the N. A. C. A. 23012 external-airfoil flap set at angles of −3° (upright and inverted) and 30° appear in figures 19 to 21. Important characteristics of the two airfoil-flap combinations tested in the variable-density tunnel are summarized in table I.

previously mentioned constants have been selected to give reasonably good agreement with the test results at moderate positive and negative angles of attack. The characteristic curves may be faired together at zero lift, giving preference to the positive-angle data; or the positive-angle data may be employed in the immediate neighborhood of zero lift.

Discussion of airfoil characteristics.—The high values of the maximum lift coefficient obtained, 2.37 for the N. A. C. A. 23012 airfoil with flap and 2.41 for the N. A. C. A. 23021 airfoil with flap at an effective Reynolds Number of about 8,000,000, compare favorably with those obtained for most other high-lift devices.

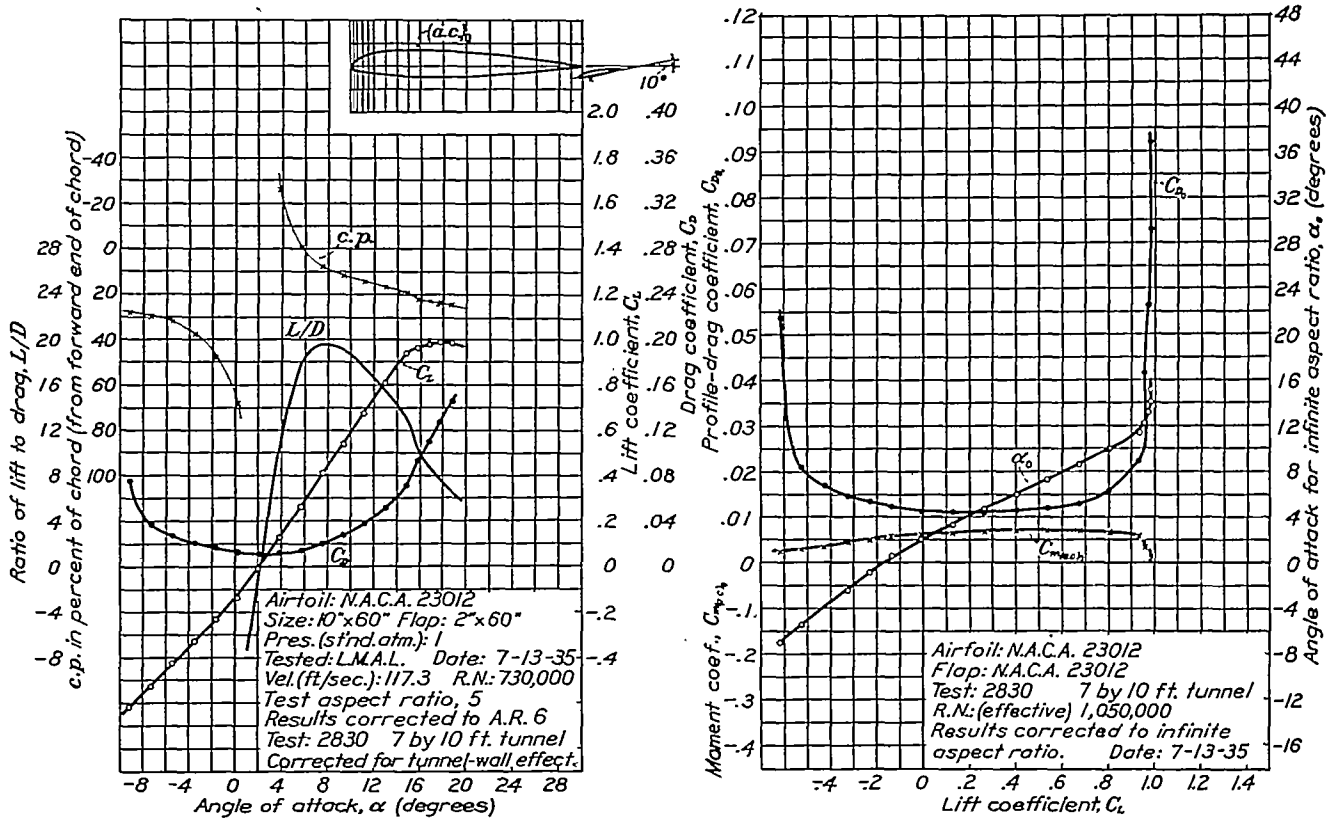

FIGURE 5.—The N. A. C. A. 23012 airfoil with $0.20c_w$ N. A. C. A. 23012 external-airfoil flap. Flap angle, −10°. The airfoil is the same as used for test 2831-a (fig. 6), except the flap setting. The value of $C_{m_{(a.c.)_0}}$ is computed about the aerodynamic center used for test 2831-a.

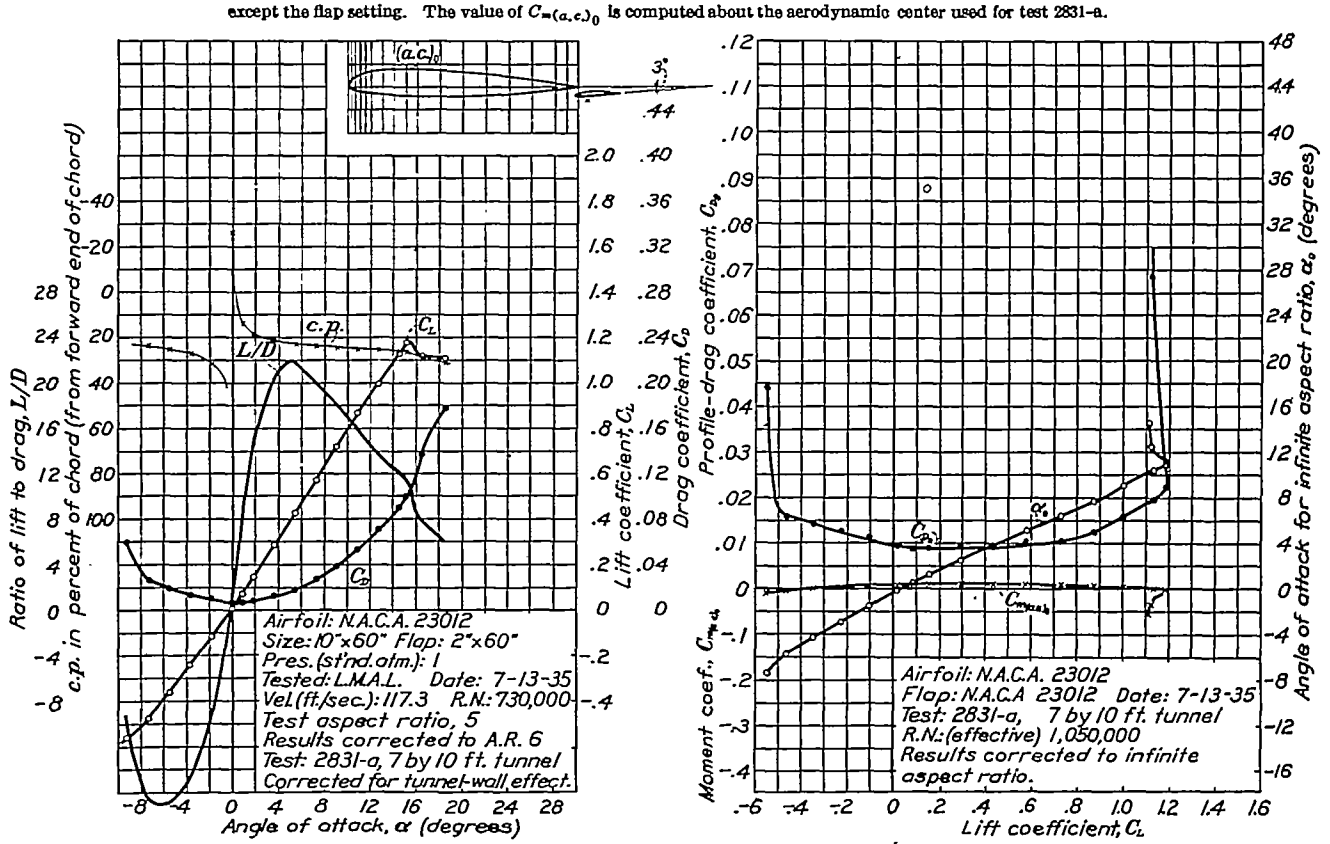

Flap angle		−3°	
Main wing section	N. A. C. A. 23012		
Flap section	N. A. C. A. 23012		
Main wing chord, c_w		0.833c	
Flap chord, $c_f = 0.2c_w$		.1667c	
Datum chord, $c = c_w + c_f$			
Pivot aft trailing edge of c_w	0.032c_w	.0268c	
Pivot below main wing chord	.054c_w	.045c	
Pivot aft. flap leading edge	0.25c_f	0.0417c	
Pivot below flap chord	.10c_f	.0167c	
Flap displacement angle		−3°	
$(a.c.)_0$ from leading edge		.245c	
$(a.c.)_0$ above main wing chord		.08	
$(a.c.)_0$ same as for variable-density tunnel test 1273 (fig. 14) without correction for effect of rectangular tips.			

FIGURE 6.—The N. A. C. A. 23012 airfoil with $0.20c_w$ N. A. C. A. 23012 external-airfoil flap.

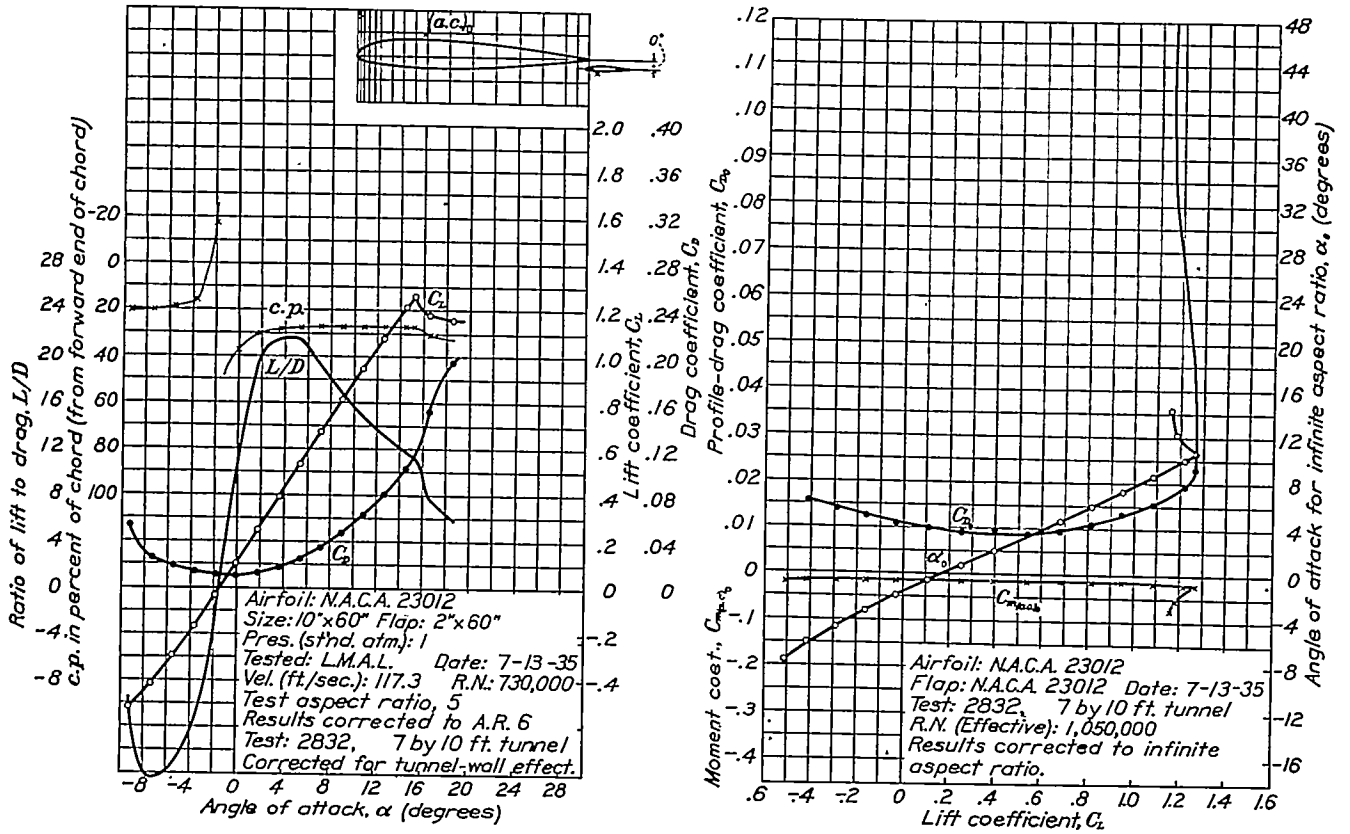

FIGURE 7.—The N. A. C. A. 23012 airfoil with 0.20c_w N. A. C. A. 23012 external-airfoil flap. Flap angle, 0°. The airfoil is the same as used for test 2831-a (fig. 6) except the flap setting. The value of $C_{m_{(a.c.)_0}}$ is computed about the aerodynamic center used for test 2831-a.

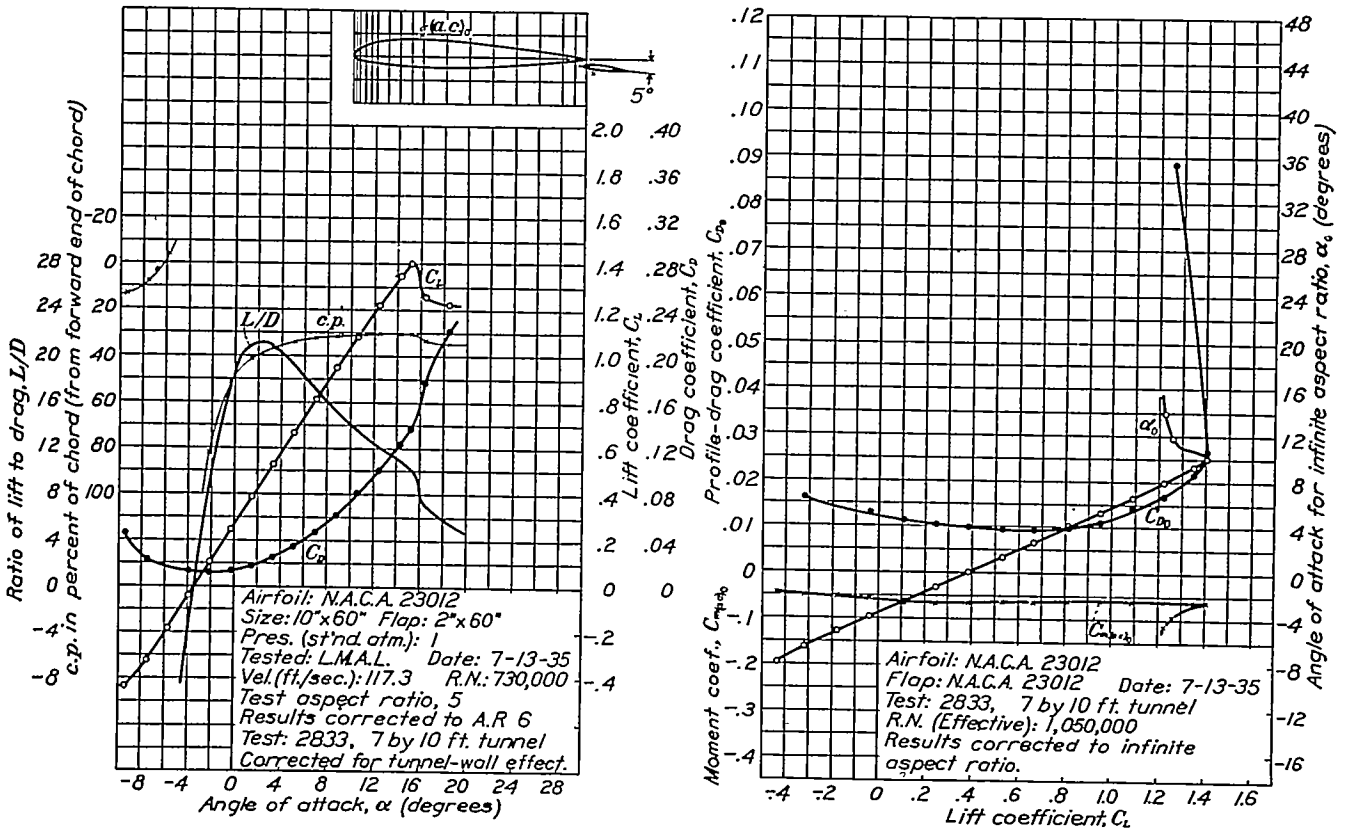

FIGURE 8.—The N. A. C. A. 23012 airfoil with 0.20c_w N. A. C. A. 23012 external-airfoil flap. Flap angle, 5°. The airfoil is the same as used for test 2831-a (fig. 6), except the flap setting. The value of $C_{m_{(a.c.)_0}}$ is computed about the aerodynamic center used for test 2831-a.

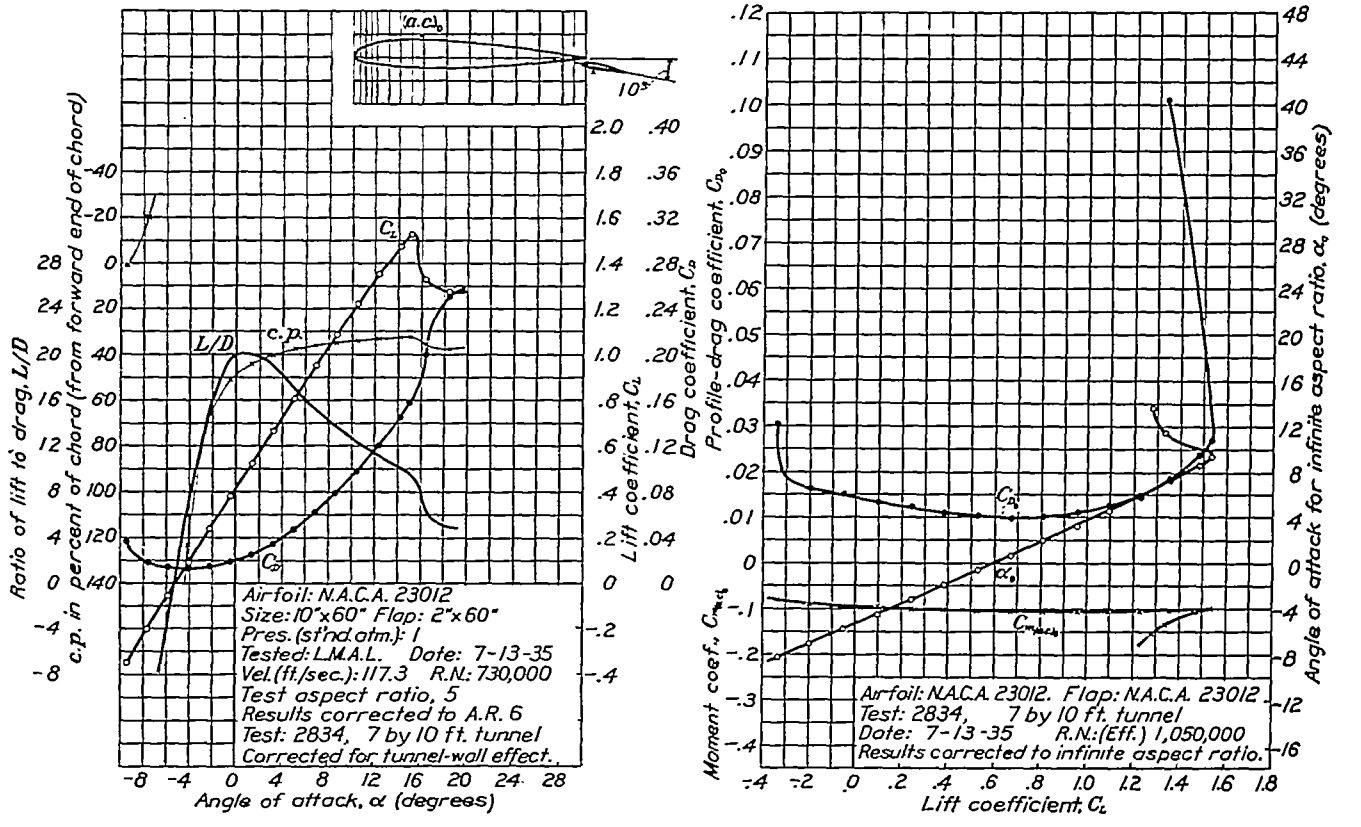

FIGURE 9.—The N. A. C. A. 23012 airfoil with 0.20c_w N. A. C. A. 23012 external-airfoil flap. Flap angle, 10°. The airfoil is the same as used for test 2831-a (fig. 6), except the flap setting. The value of $C_{m_{(a.c.)_0}}$ is computed about the aerodynamic center used for test 2831-a.

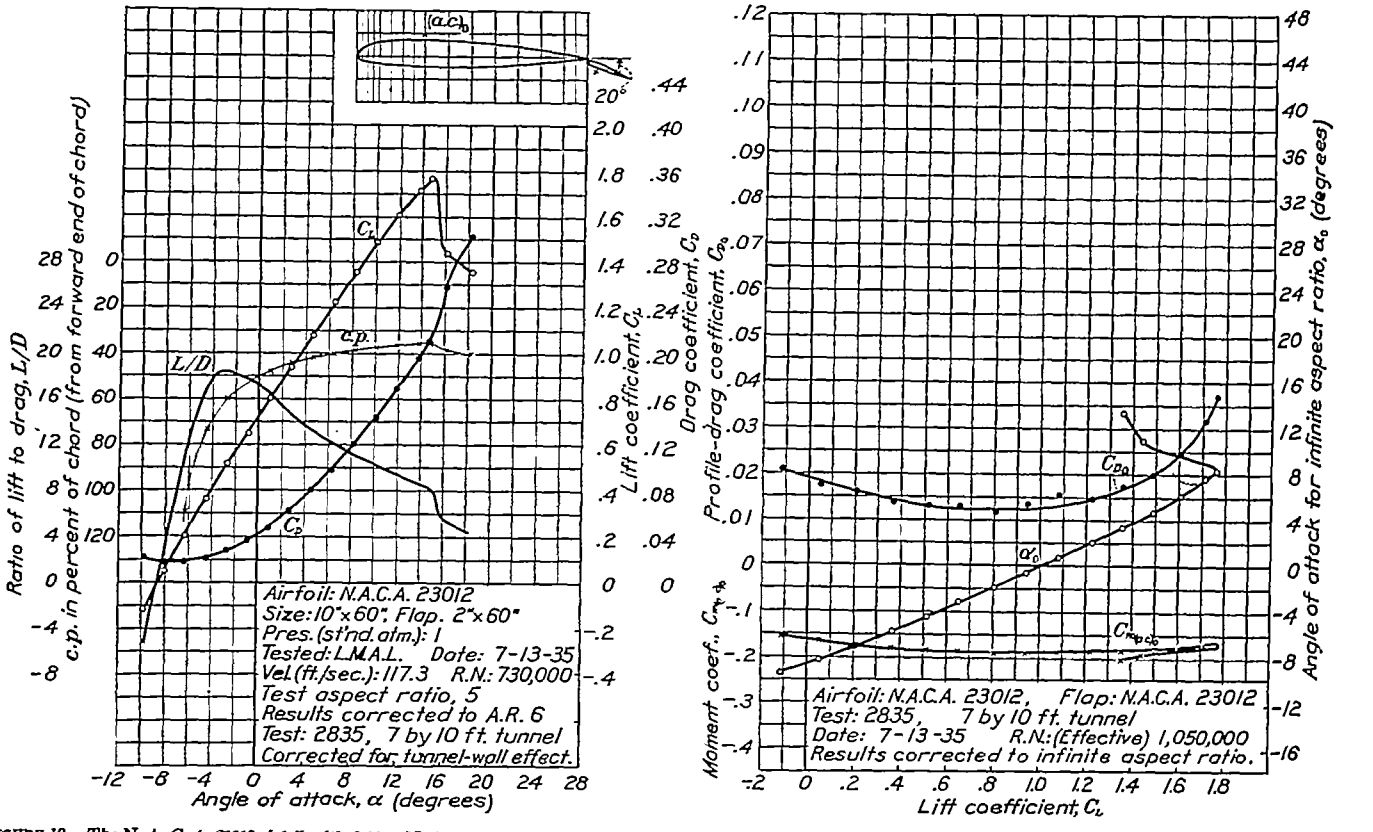

FIGURE 10.—The N. A. C. A. 23012 airfoil with 0.20c_w N. A. C. A. 23012 external-airfoil flap. Flap angle, 20°. The airfoil is the same as used for test 2831-a (fig. 6), except the flap setting. The value of $C_{m_{(a.c.)_0}}$ is computed about the aerodynamic center used for test 2831-a.

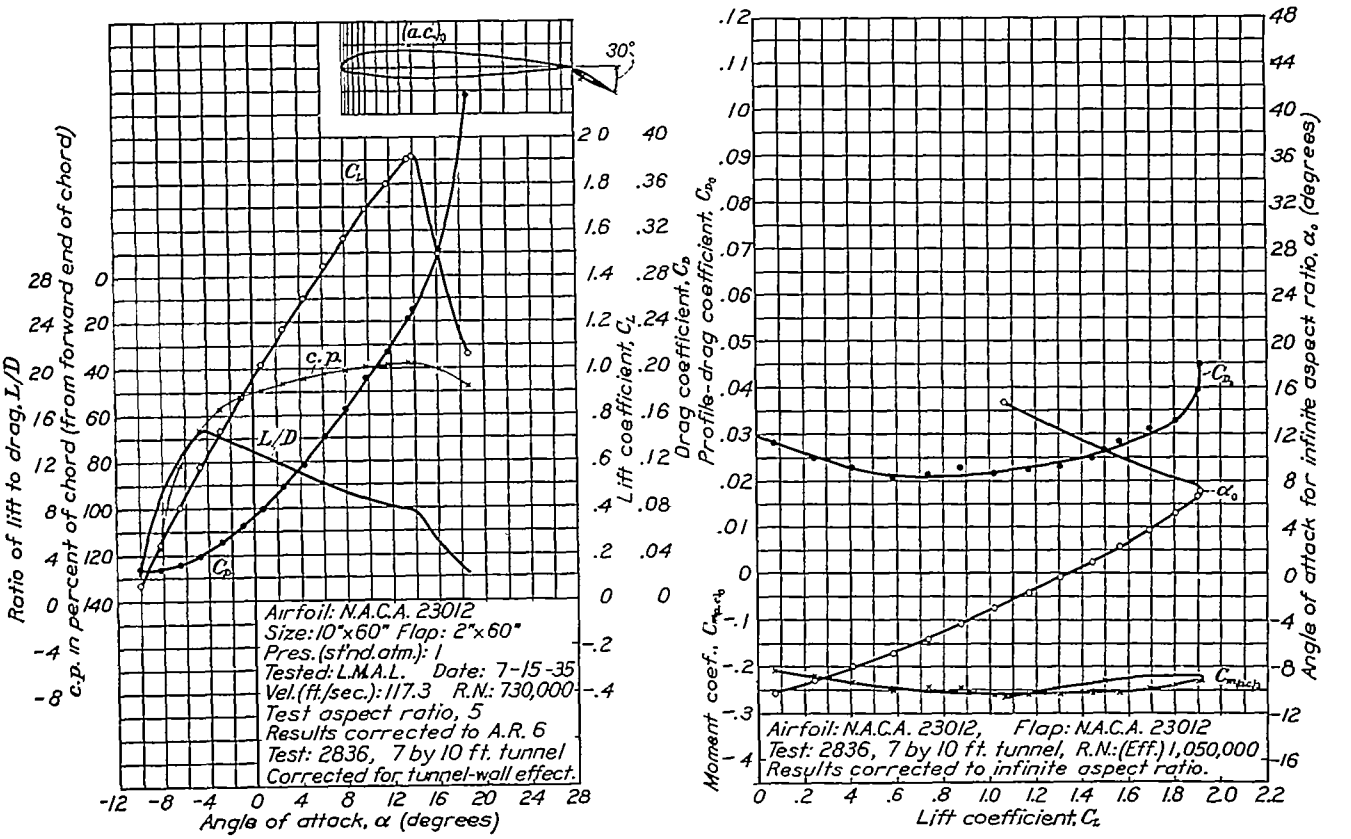

FIGURE 11.—The N. A. C. A. 23012 airfoil with 0.20c_w N. A. C. A. 23012 external-airfoil flap. Flap angle, 30°. The airfoil is the same as used for test 2831-a (fig. 6) except the flap setting. The value of $C_{m_{(a.c.)_0}}$ is computed about the aerodynamic center used for test 2831-a.

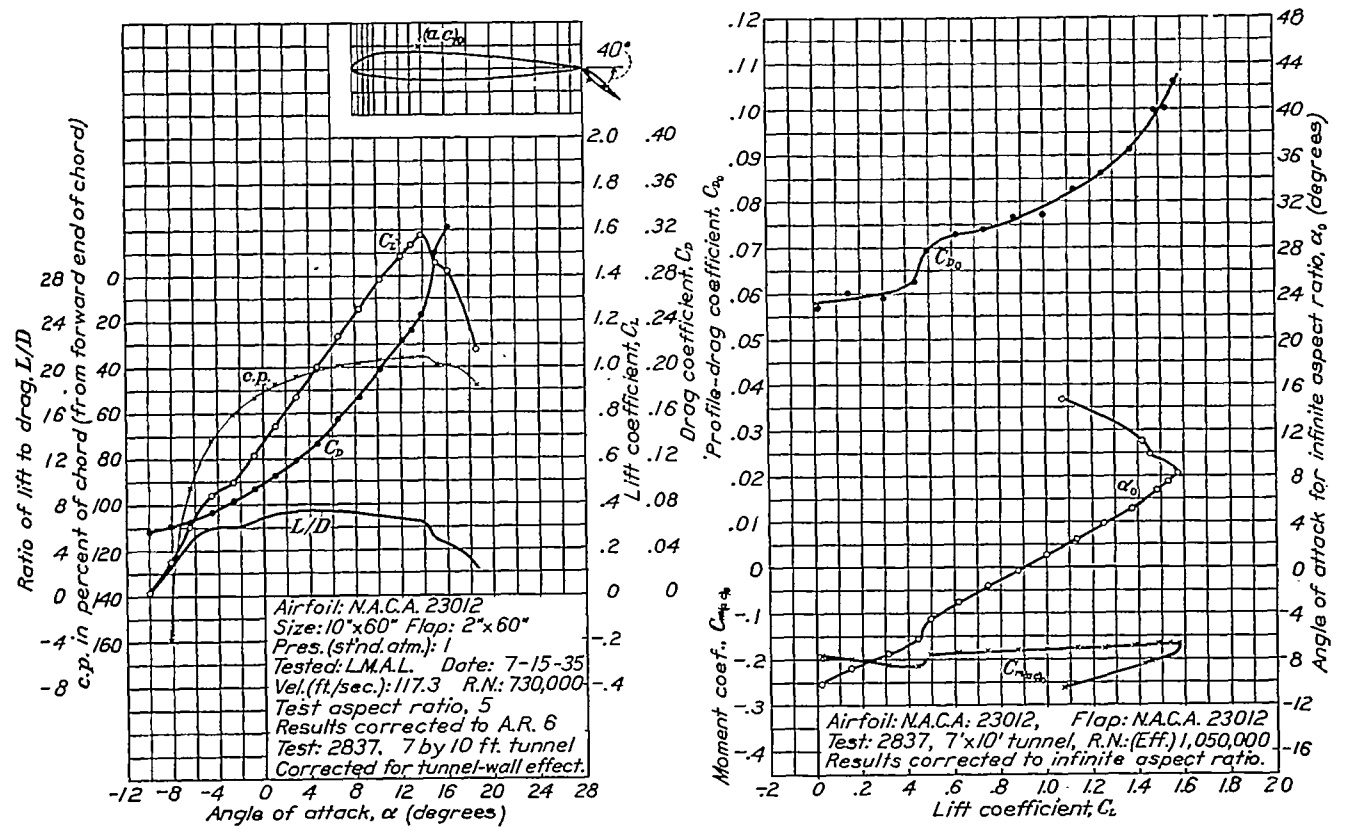

FIGURE 12.—The N. A. C. A. 23012 airfoil with 0.20c_w N. A. C. A. 23012 external-airfoil flap. Flap angle, 40°. The airfoil is the same as used for test 2831-a (fig. 6) except the flap setting. The value of $C_{m_{(a.c.)_0}}$ is computed about the aerodynamic center used for test 2831-a.

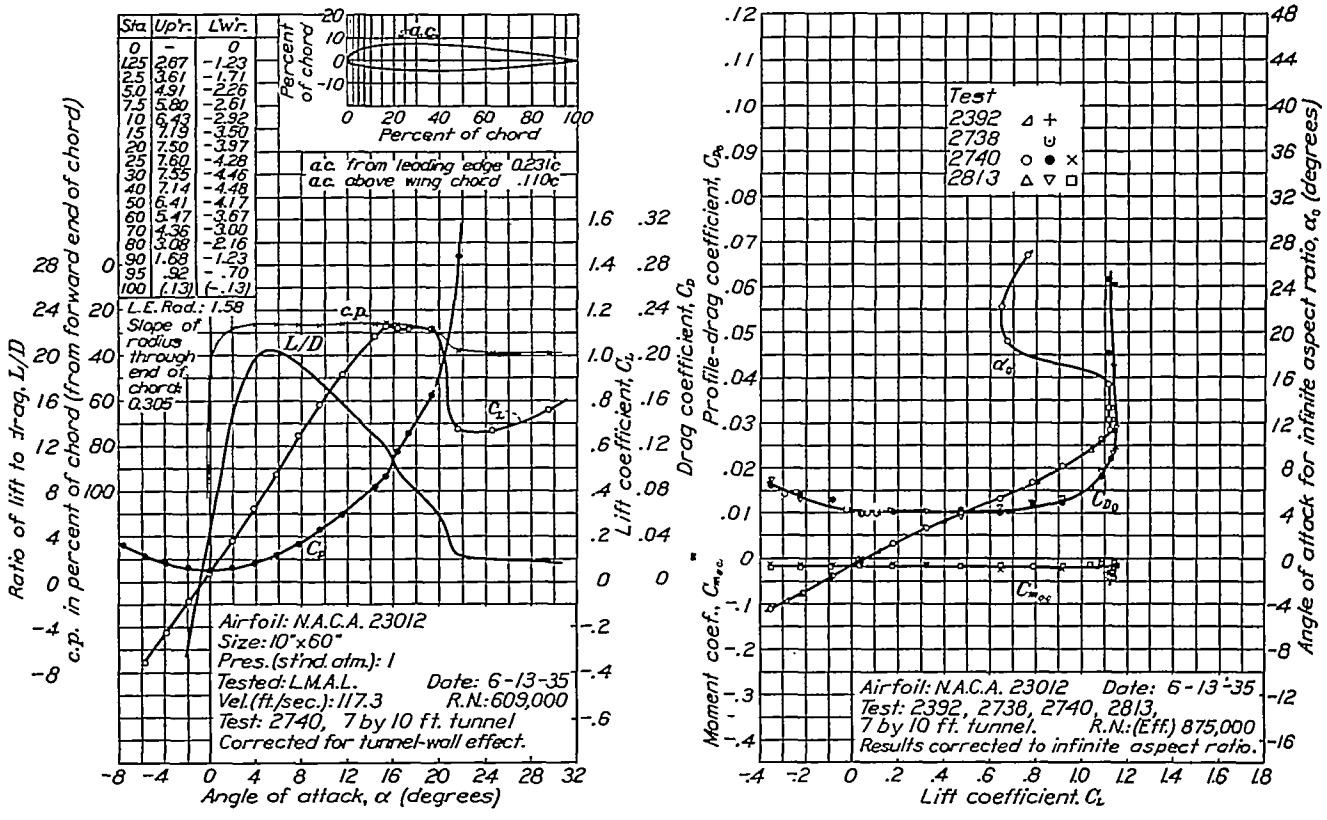

FIGURE 13.—The N. A. C. A. 23012 airfoil.

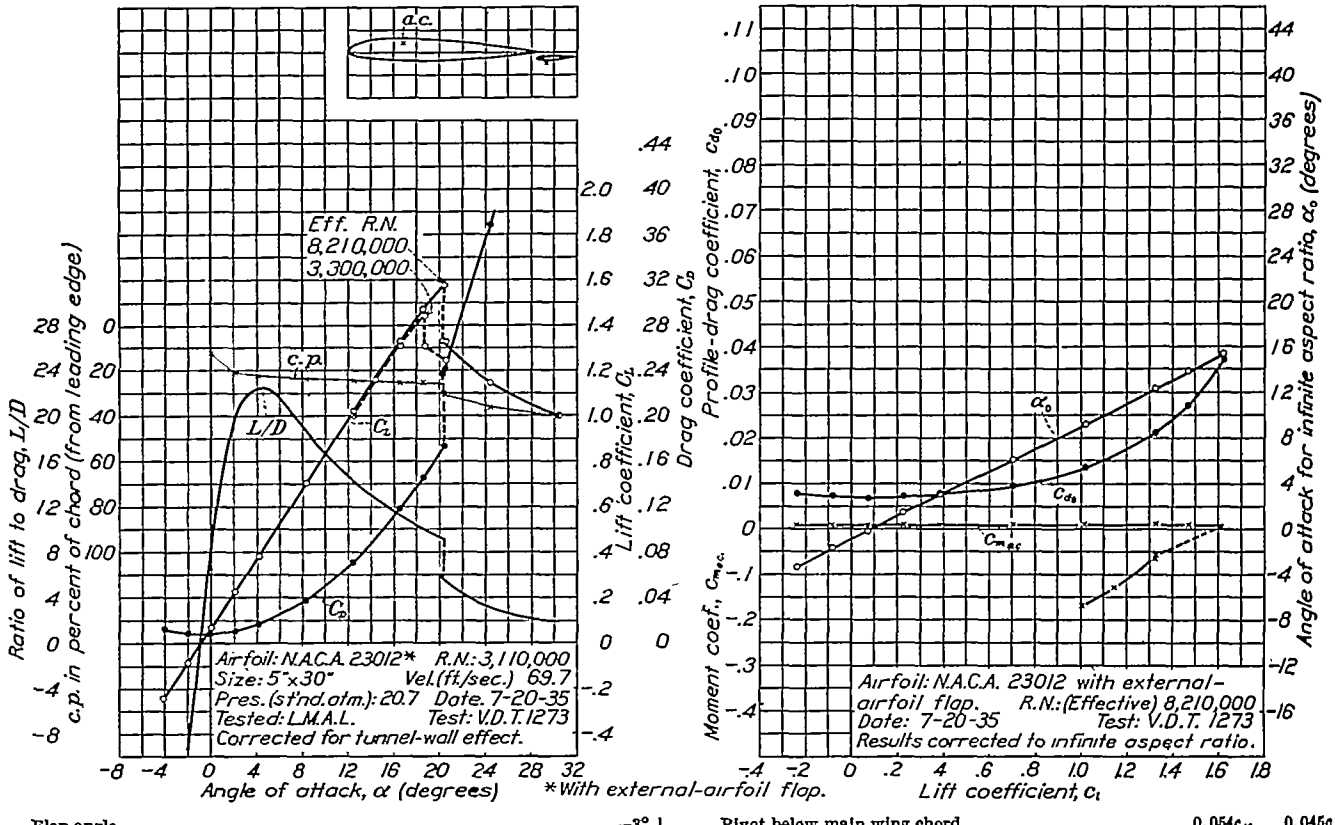

Flap angle	−3°		
Main wing section	N. A. C. A. 23012		
Flap section	N. A. C. A. 23012		
Main wing chord, c_w	0.833c		
Flap chord, $c_f=0.2c_w$	.1667c		
Datum chord, $c=c_w+c_f$			
Pivot aft trailing edge of c_w	0.03c_w	.025c	
Pivot below main wing chord	0.054c_w	0.045c	
Pivot aft flap leading edge	.24c_f	.040c	
Pivot below flap chord	.10c_f	.0107c	
Flap displacement angle		1-3°	
a. c. from leading edge		.240c	
a. c. above main wing chord		.04c	

FIGURE 14.—The N. A. C. A. 23012 airfoil with 0.20c_w N. A. C. A. 23012 external-airfoil flap.

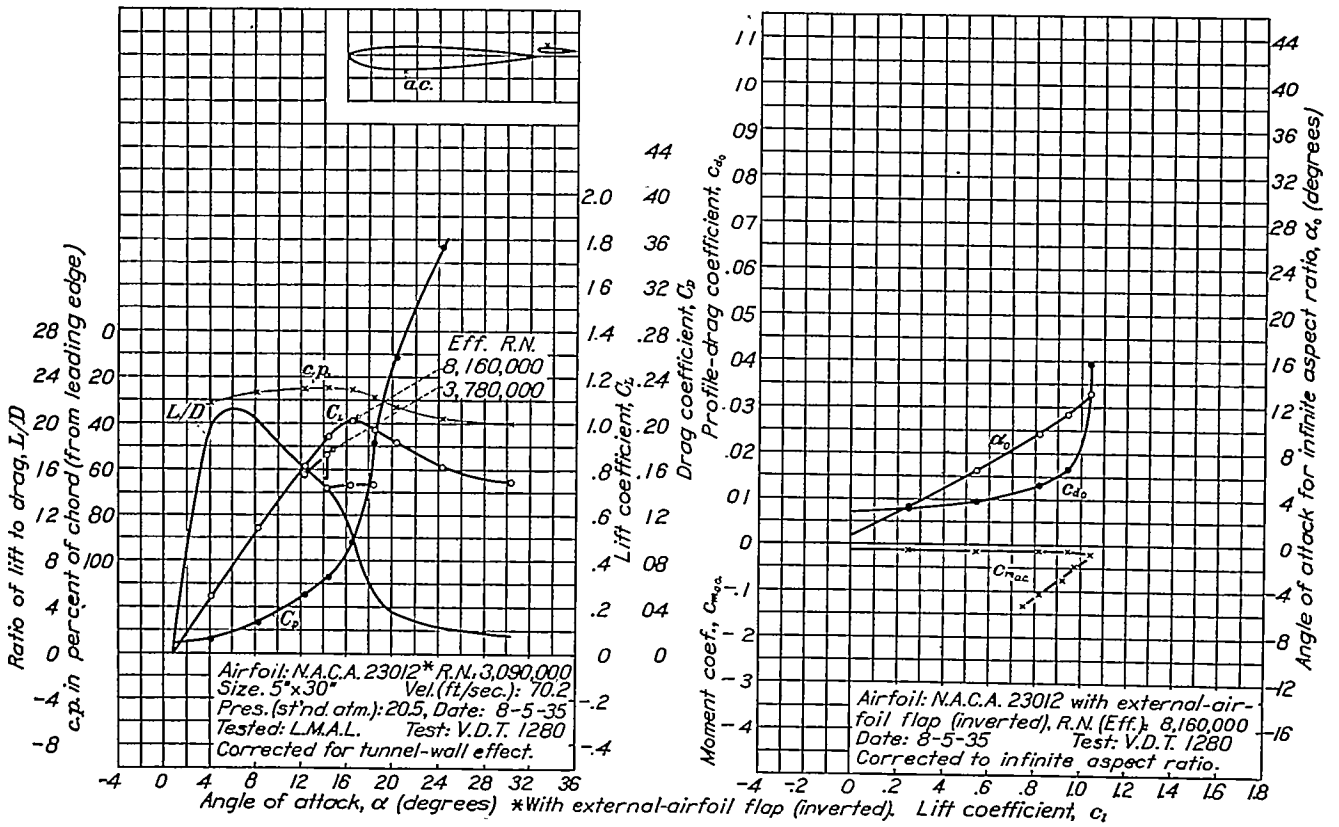

FIGURE 15.—The N. A. C. A. 23012 airfoil with 0.20c_w N. A. C. A. 23012 external-airfoil flap. Flap angle, −3°. The airfoil is the same as used for variable-density tunnel test 1273 (fig. 14) except inverted; *a. c.* from leading edge, 0.252*c*; *a. c.* above main wing chord, −0.07*c*.

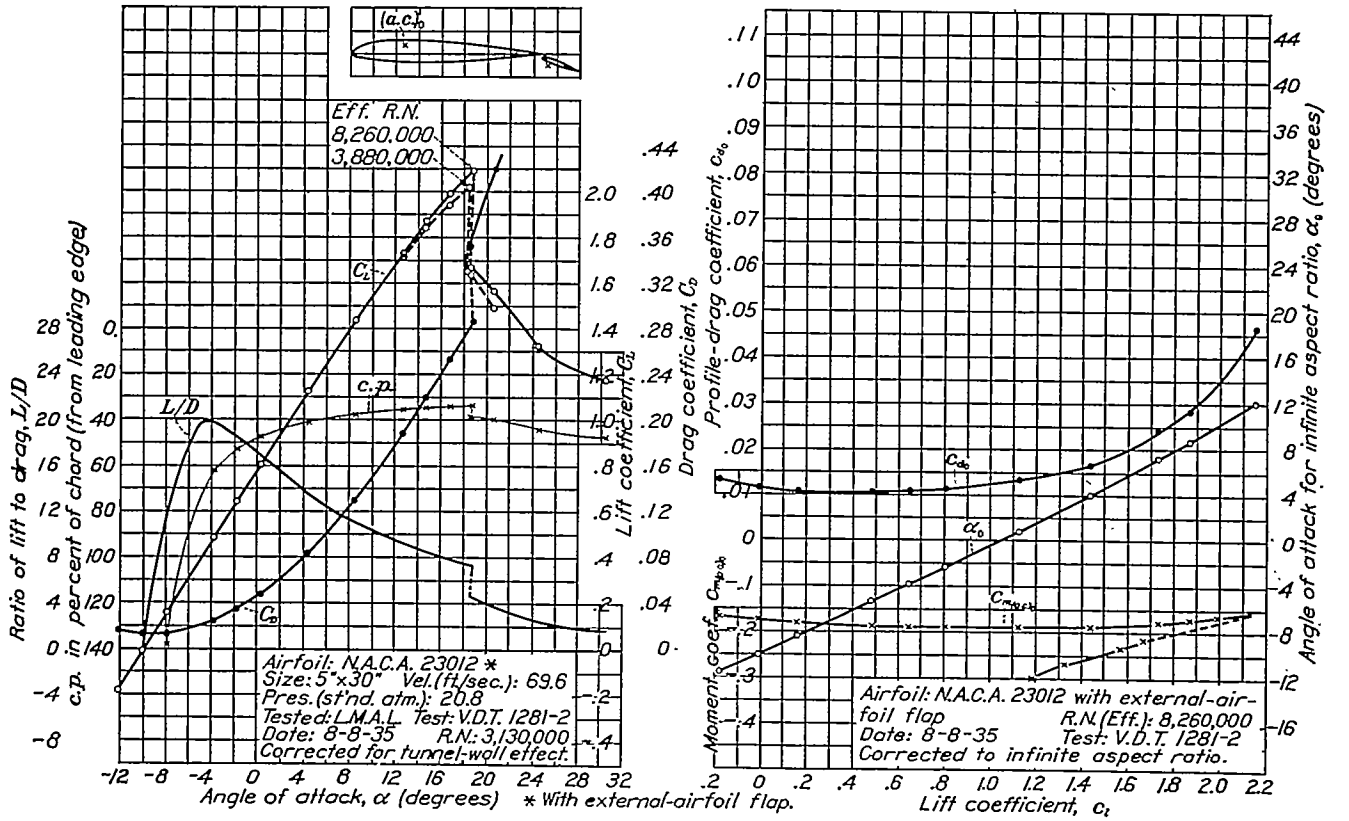

FIGURE 16.—The N. A. C. A. 23012 airfoil with 0.20c_w N. A. C. A. 23012 external-airfoil flap. Flap angle, 20°. The airfoil is the same as used for variable-density tunnel test 1273 (fig. 14) except the flap setting. The value of $c_{m_{(a.c.)_0}}$ is computed about the aerodynamic center as determined for test 1273.

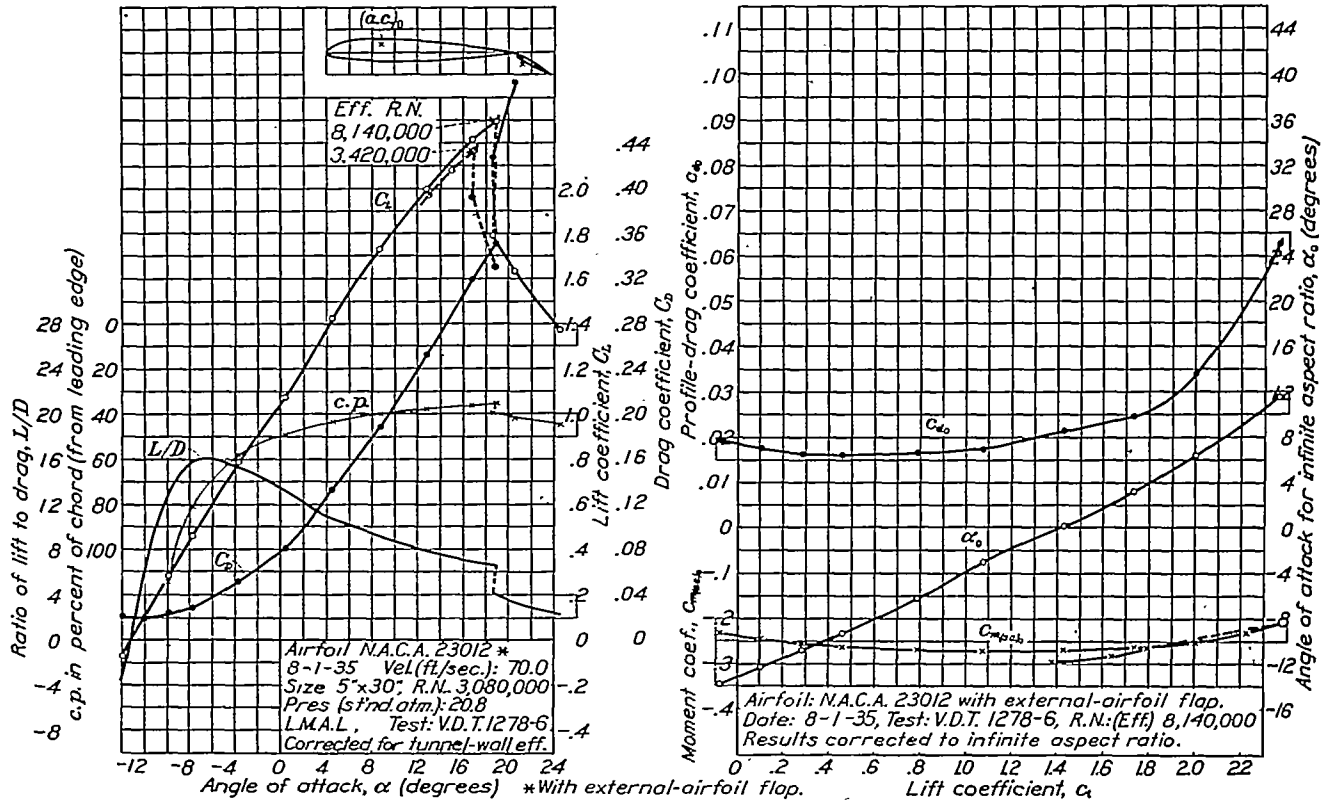

FIGURE 17.—The N. A. C. A. 23012 airfoil with 0.20c_w N. A. C. A. 23012 external-airfoil flap. Flap angle, 30°. The airfoil is the same as used for variable-density tunnel test 1273 (fig. 14) except the flap setting. The value of $c_{m_{(a.c.)_0}}$ is computed about the aerodynamic center as determined for test 1273.

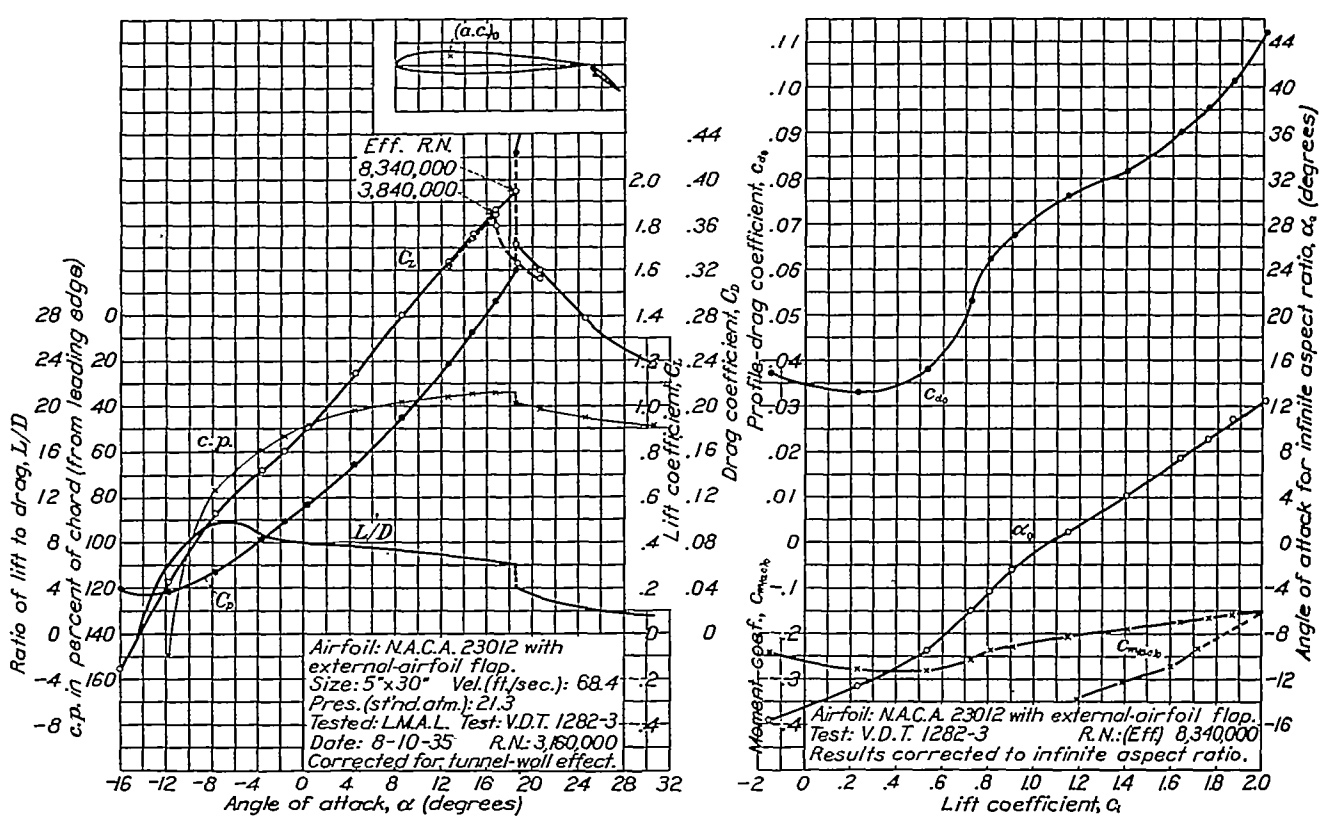

FIGURE 18.—The N. A. C. A. 23012 airfoil with 0.20c_w N. A. C. A. 23012 external-airfoil flap. Flap angle, 40°. The airfoil is the same as used for variable-density tunnel test 1273 (fig. 14) except the flap setting. The value of $c_{m_{(a.c.)_0}}$ is computed about the aerodynamic center as determined for test 1273.

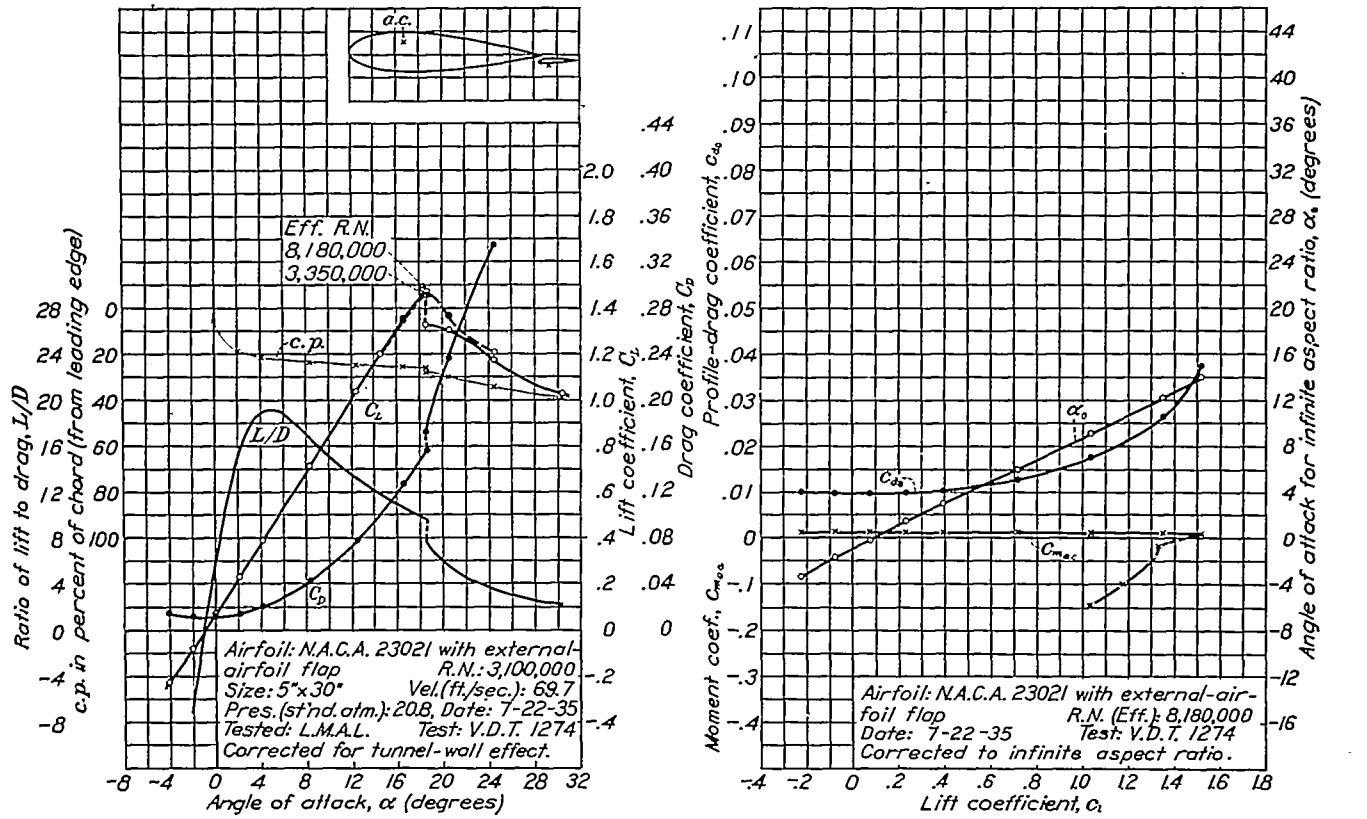

Flap angle	−3°	
Main wing section	N. A. C. A. 23021	
Flap section	N. A. C. A. 23012	
Main wing chord, c_w	0.833c	
Flap chord, $c_f=0.2c_w$	.1667c	
Datum chord, $c=c_w+c_f$		
Pivot aft trailing edge of c_w	0.03c_w	.026c
Pivot below main wing chord	0.054c_w	0.045c
Pivot aft flap leading edge	.24c_f	.040c
Pivot below flap chord	.10c_f	.0167
Flap displacement angle		−3°
a. c. from leading edge		.239c
a. c. above main wing chord		.06c

FIGURE 19.—The N. A. C. A. 23021 airfoil with 0.20 c_w N. A. C. A. 23012 external-airfoil flap.

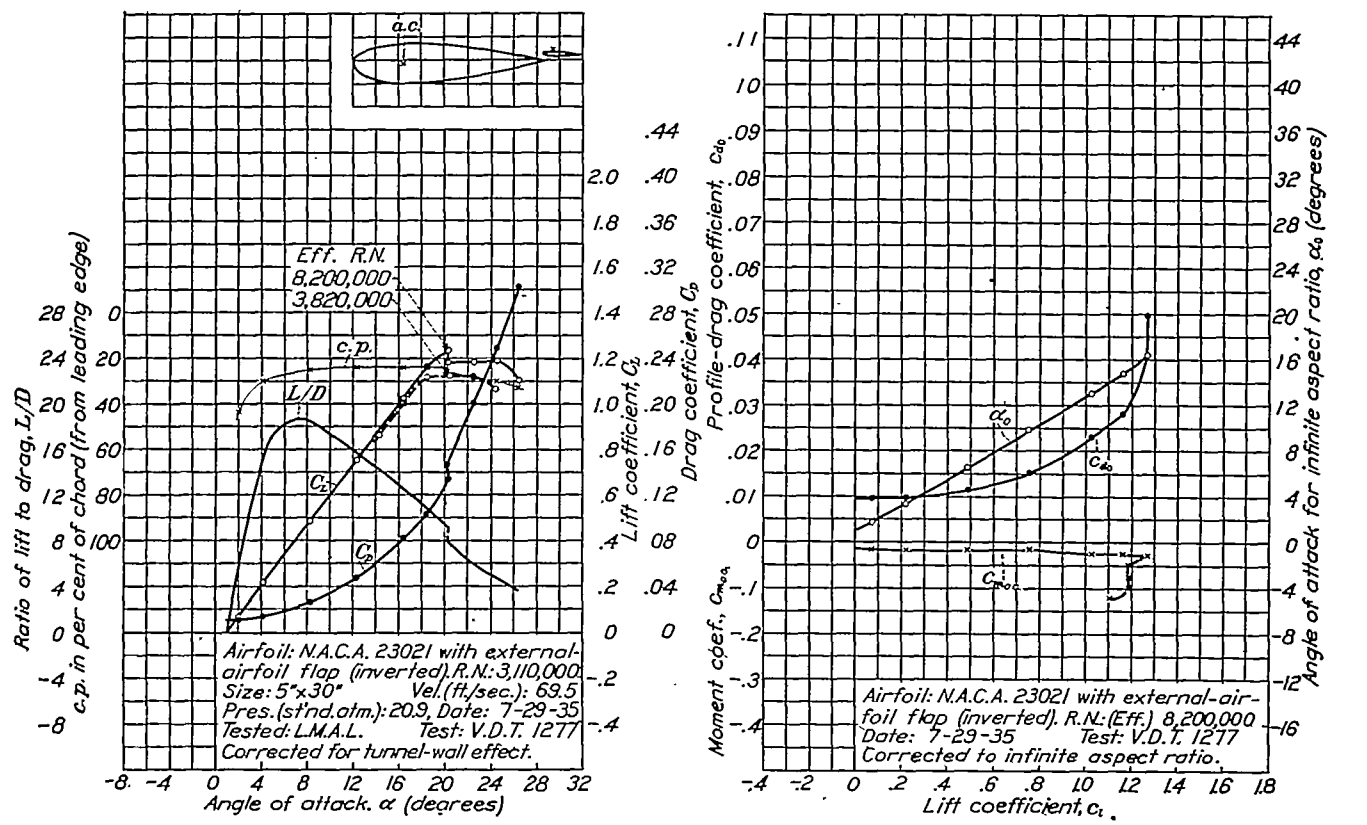

FIGURE 20.—The N. A. C. A. 23021 airfoil with 0.20c_w N. A. C. A. 23012 external-airfoil flap. Flap angle, −3°. The airfoil is the same as used for variable-density tunnel test 1274 (fig. 19) except inverted; a. c. from leading edge, 0.217c; a. c. above main wing chord, −0.01c.

The minimum drag coefficients obtained for both airfoil-flap combinations indicate a slight favorable interference between the airfoil and the flap. The values obtained at an effective Reynolds Number of about 8,000,000 were 0.0069 and 0.0097, respectively, for the combinations using the N. A. C. A. 23012 and the N. A. C. A. 23021 airfoils for the main airfoil sections. These values are lower than those obtained for the N. A. C. A. 23012 and the N. A. C. A. 23021 sections alone, which have minimum drag coefficients of 0.0071 and 0.0101, respectively (reference 10). Airfoils of the N. A. C. A. 230 series of lower thickness ratios having the same maximum thickness for the same chord as the combination tested afford, however, curves show the effects of scale on the characteristics plotted. It will be noted that the scale-effect curve for the maximum lift coefficient of the N. A. C. A. 23012 airfoil-flap combination as determined in the variable-density wind tunnel has a discontinuity at an effective Reynolds Number of about 1,700,000. The point obtained in the 7- by 10-foot wind tunnel at an effective Reynolds Number of only 1,000,000, however, lies on the extension of the curve obtained in the variable-density wind tunnel at higher Reynolds Numbers. Only two points were obtained for the combination using the N. A. C. A. 23021 section for the main airfoil in the variable-density tunnel, but for this case also it appears that a similar discontinuity may

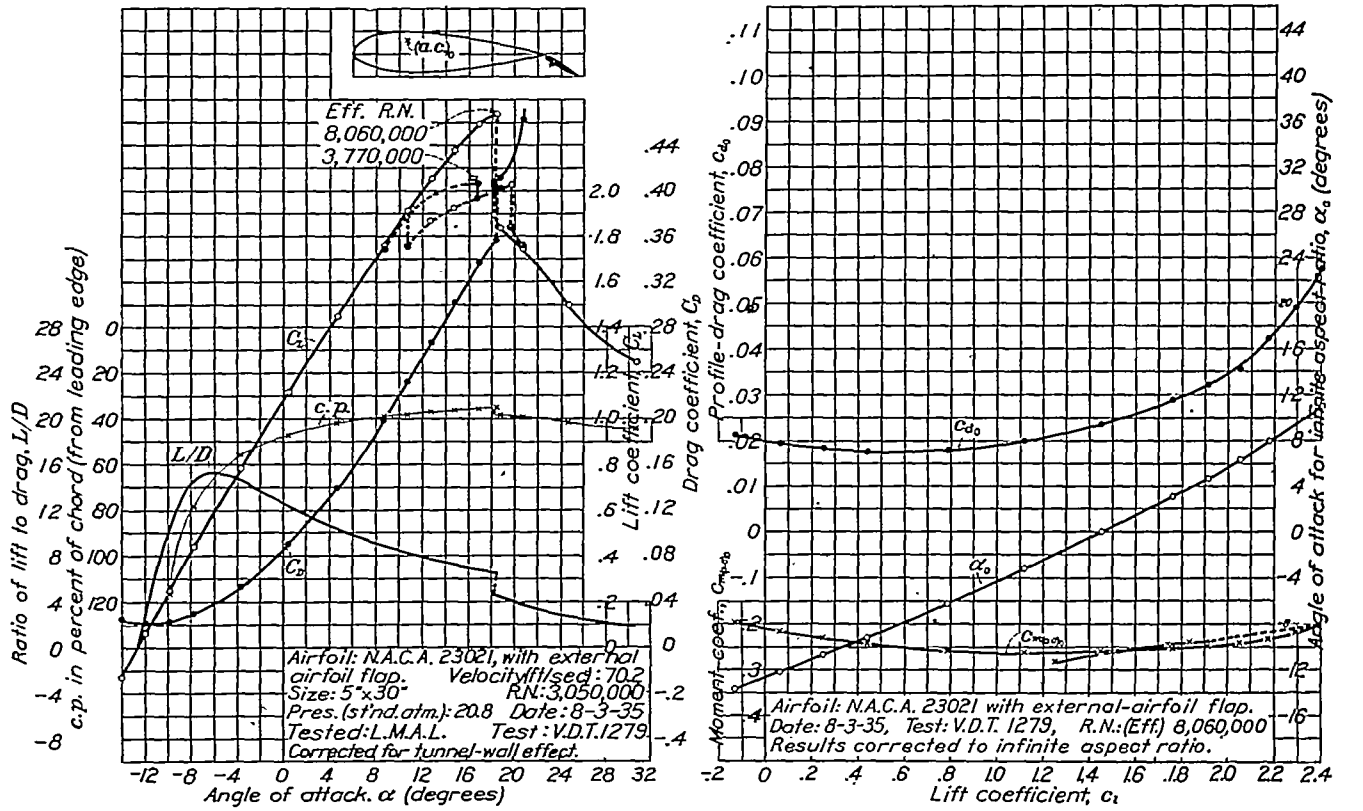

FIGURE 21.—The N. A. C. A. 23021 airfoil with 0.20c_w N. A. C. A. 23012 external-airfoil flap. Flap angle, 30°. The airfoil is the same as used for variable-density tunnel test 1274 (fig. 19) except the flap setting. The value of $c_{m_{(a.c.)_0}}$ is computed about the aerodynamic center as determined for test 1274.

a better comparison. One such section is the N. A. C. A. 23010 predicted to have a minimum drag coefficient of 0.0067 and another is the N. A. C. A. 23018, which has a minimum drag coefficient of 0.0091 (reference 10). These values are slightly lower than those obtained with the comparable wing-flap combinations.

The variations of maximum lift and minimum drag coefficient with effective Reynolds Number are shown in figure 22. The data plotted in this figure are not corrected for hinge tares or for the effects of rectangular tips because these corrections were not known with certainty at all values of the effective Reynolds Number. The values plotted differ, therefore, from the fully corrected values given elsewhere, but the exist, as evidenced by the low maximum lift coefficient obtained at an effective Reynolds Number of 3,800,000.

An explanation of this phenomenon and the apparent difference between the results from the two tunnels is indicated by the fact that the observed discontinuity tends to appear at a constant value of the test Reynolds Number rather than of the effective Reynolds Number. As pointed out in reference 8, the concept of effective Reynolds Number is applicable only when the scale effect is determined mainly by the influence of the transition from a laminar to a turbulent boundary layer. In the present case the flow through the slot probably is the important factor and depends upon the boundary-layer thickness relative to the slot size, which in turn is more nearly dependent on the

test Reynolds Number than on the effective Reynolds Number. Interpreted on this basis, the apparent conflict between the results obtained in the variable-density and the 7- by 10-foot wind tunnels disappears, and it is probable that wings in flight will show the discontinuity, if at all, at values of the Reynolds Number lower than the effective values at which the discontinuities occur in the variable-density tunnel.

The scale effect on minimum profile drag, as shown in figure 22, is about the same for both combinations.

Flap loads.—The variation of flap normal force, flap chord force, and flap center of pressure, with lift coefficient of the airfoil-flap combination is shown in figure 23. These data are in no case extended to the maximum lift coefficient of the combination at the flap angle in question on account of erratic points obtained in the tests. The data indicated that, with the flap supported separately, either the main airfoil or the flap had a tendency to stall prematurely, rendering the values in the region of $C_{L_{max}}$ inconsistent and unreliable.

The variation of flap hinge-moment coefficient C_{H_f} with flap angle about the two hinge-axis locations used is shown in figures 24 and 25. It will be noted that the flap is slightly overbalanced between angles of −5° and −10° when hinged at axis 1. Although the overbalance does not occur in the normal flap-operating range (−3° to 30°), it seems likely that overbalance might occur in operation of the flaps as ailerons with a neutral setting of −3°. For this reason the second location, axis 2 (fig. 1), was selected and used for further hinge-moment tests. This hinge axis is exactly 1 percent of the flap chord ahead of axis 1. Even with this axis, some slight degree of overbalance remains although it is considerably less than that encountered with axis 1 and is not considered likely to cause aileron overbalance in the high-speed condition.

Since the tests in the variable-density tunnel were based on the results of the 7- by 10-foot wind-tunnel tests, it was considered desirable to use flap hinge axis 2, which seems slightly more satisfactory than 1, in the variable-density-tunnel tests. Inasmuch as the flap was hinged at axis 1 for the 7- by 10-foot wind-tunnel tests, there is a slight discrepancy of flap position between the final force tests in the two tunnels. The rate of variation of lift and drag characteristics with flap position, as shown in figure 4, indicates, however, that the effect of this difference on the final force-test data may be regarded as negligible.

General features of combinations of airfoil and external-airfoil flap.—The present external-airfoil flap combinations appear to have as many desirable aerodynamic characteristics as other good high-lift devices tested up to the present. They give a high maximum lift coefficient and a low minimum drag coefficient; in these respects, however, their merit is approximately equal to that of such a device as the split flap. At the same time they give a much lower value of drag coefficient throughout the high-lift range, provided that the flap is set at the proper angle, than do split flaps. If a large drag at a high lift coefficient is desired to obtain steep gliding ability, characteristics approaching those of the split flap can be obtained by deflecting the external-airfoil flap to larger angles than the optimum, thus causing the flap to stall and to give large increases of profile drag. A different hinge axis, selected with this characteristic in mind, should give large available values of profile drag at high lift coefficients without entailing much increase in the minimum values of profile drag obtainable throughout the lift range.

Another feature of external-airfoil flaps is the possibility of deflecting them as ailerons, while they cover the full span of the wing as a high-lift device. As explained in reference 1, disadvantages in connection with overbalance when the ailerons are deflected differentially and with large values of adverse yawing

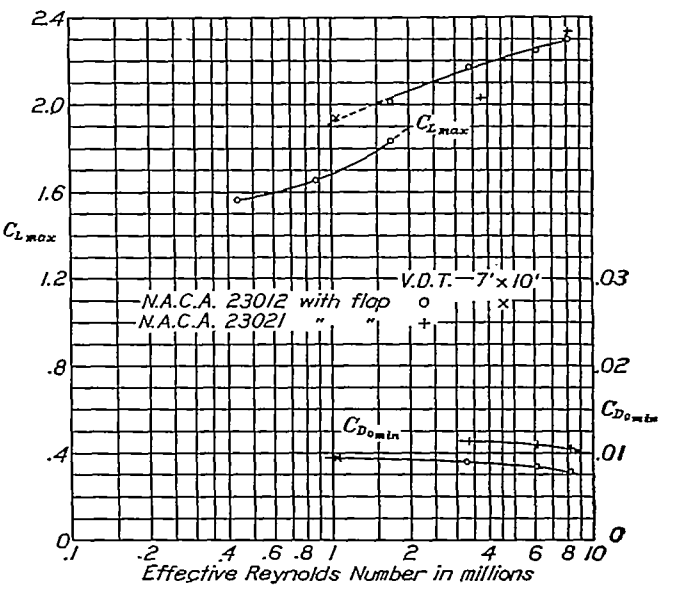

FIGURE 22.—Scale effect on N. A. C. A. 23012 and N. A. C. A. 23021 airfoils with 0.20c_m N. A. C. A. 23012 external-airfoil flap. All values uncorrected for hinge tares and for effects of rectangular tips.

moment render their value as a lateral-control arrangement doubtful. Unfortunately the use of the full-span flap for glide control, as suggested previously, is incompatible with its use as a lateral-control device. An arrangement using the tip portions as combined ailerons and flaps, with the center portion capable of being deflected to much larger angles for glide control, appears to offer a possibility of combining these various features, provided that the large values of adverse yawing moment are acceptable.

With the data available at present, it is possible to determine the relative merit of the Clark Y and the N. A. C. A. 23012 airfoil sections for use as external-airfoil flaps on the N. A. C. A. 23012 main airfoil. Comparison of the results in this report with those of reference 1 indicates that the combination with the N. A. C. A. 23012 flap has appreciably lower drag

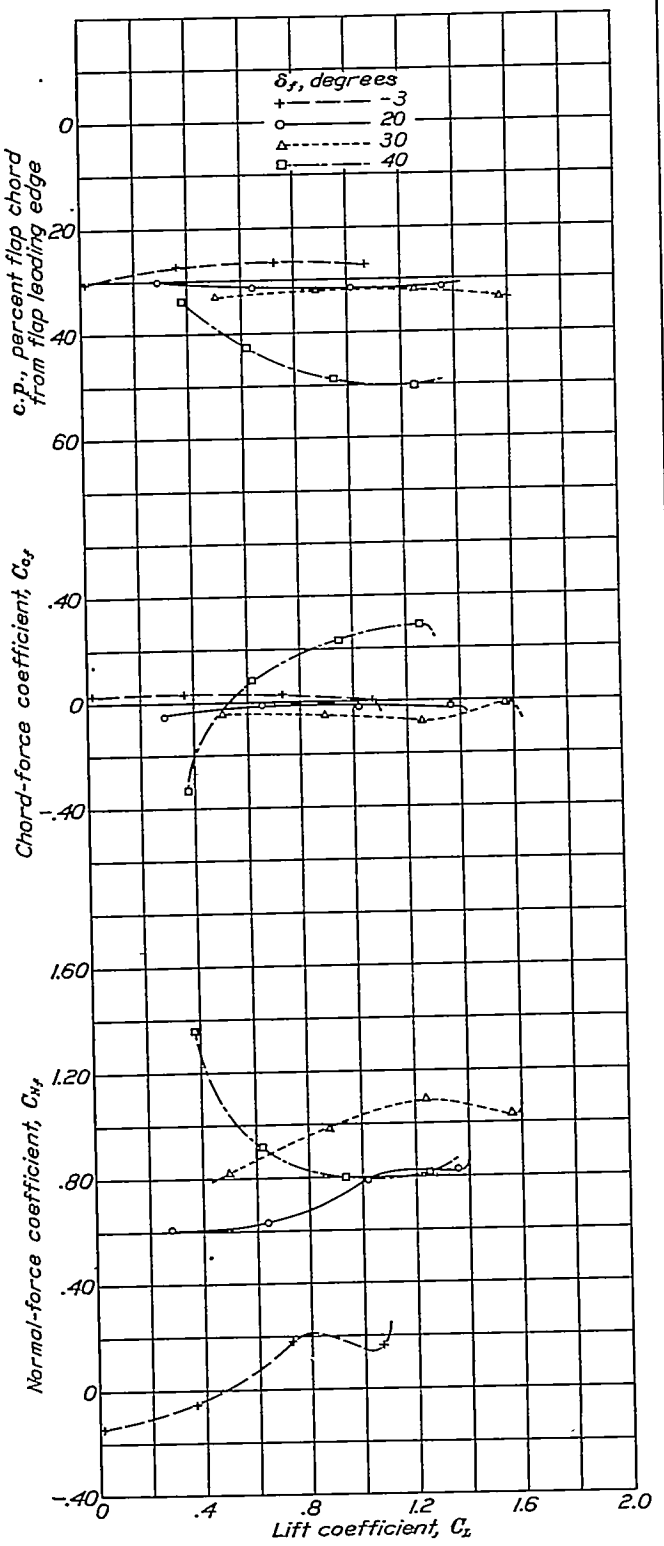

FIGURE 23.—Variation of air loads on flap with wing lift coefficient. N. A. C. A. 23012 airfoil with 0.20c_w N. A. C. A. 23012 external-airfoil flap.

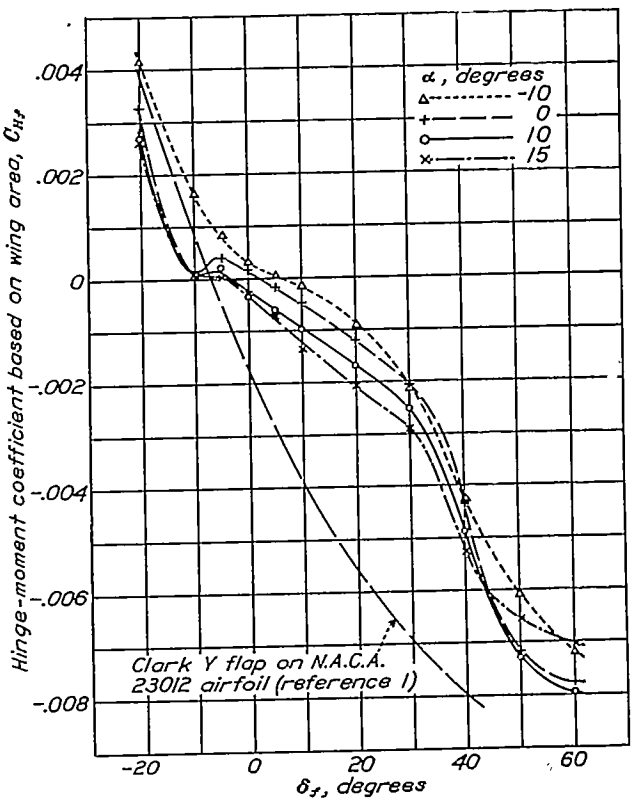

FIGURE 24.—Hinge-moment coefficients of flap. Hinge axis 1. N. A. C. A. 23012 airfoil with 0.20c_w N. A. C. A. 23012 external-airfoil flap.

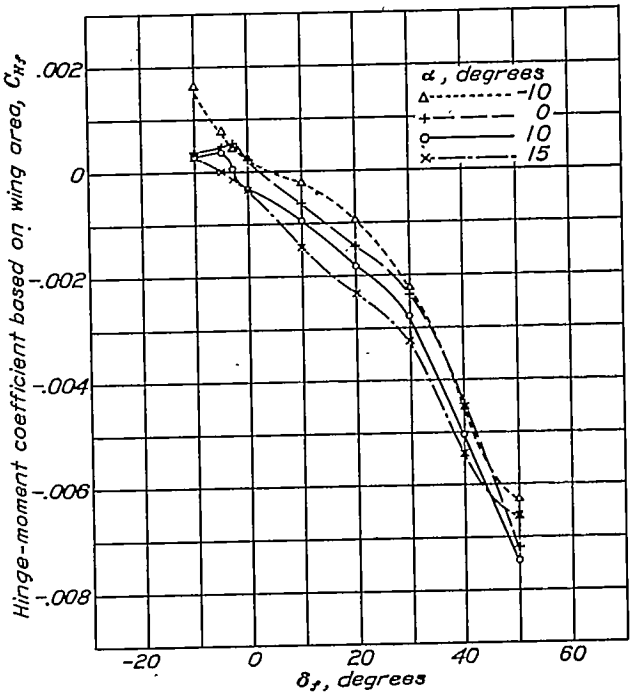

FIGURE 25.—Hinge-moment coefficients of flap. Hinge axis 2. N. A. C. A. 23012 airfoil with 0.20c_w N. A. C. A. 23012 external-airfoil flap.

throughout the whole lift range. The values obtained in the 7- by 10-foot wind tunnel of the speed-range index $C_{L_{max}}/C_{D_{min}}$, which may be considered representative of the relative merit of the two arrangements, are 192 for the N. A. C. A. 23012 flap on the N. A. C. A. 23012 airfoil and 174 for the Clark Y flap on the N. A. C. A. 23012 airfoil. Although the combination with the Clark Y flap gives a slightly higher maximum lift coefficient, it is apparent from the values of the speed-range index that the general maximum lift and minimum drag characteristics of the combination with the

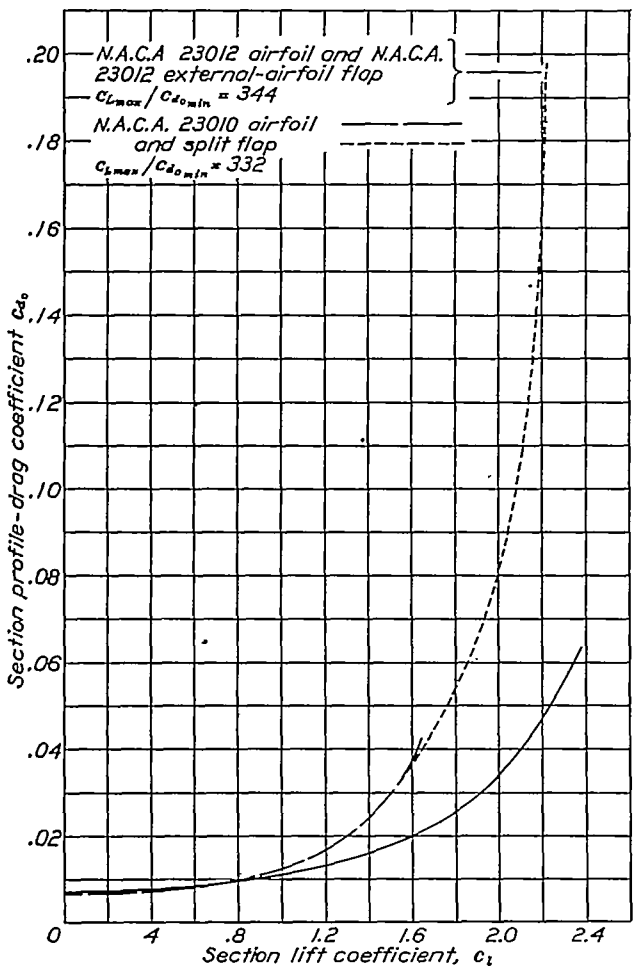

FIGURE 26.—Comparison of N. A. C. A. 23012 airfoil and 0.20c_w N. A. C. A. 23012 external-airfoil flap with N. A. C. A. 23010 airfoil and 0.20c_w split flap. Effective Reynolds Number, 8,200,000.

N. A. C. A. 23012 flap are more favorable. A study of the contour curves for maximum lift and minimum drag in this report and in reference 1 shows that the variation of optimum position of the flap with flap angle is more favorable for obtaining a hinge position giving low operating moments without sacrificing performance characteristics in the case of the N. A. C. A. 23012 flap than in the case of the Clark Y flap.

A comparison of the N. A. C. A. 23012 external-airfoil flap in combination with N. A. C. A. 23012 and N. A. C. A. 23021 airfoils, with the plain airfoils of comparable thickness equipped with split flaps is shown in figures 26 and 27. The polar curves for the flap combinations are envelope curves of the series of polars obtained at the various flap-angle settings, thus giving at each lift coefficient the minimum profile-drag coefficient obtainable from the airfoil-flap combination. The envelope curves for the split-flap combinations were constructed from data obtained from reference 11 and from unpublished tests in the variable-density tunnel. In the case of the plain airfoil equipped with a split flap, no reduction of profile-drag coefficient is obtained by deflecting the flap except at lift coefficients very near the maximum for the plain airfoil. The curves, therefore, show also the comparison of the external-flap device with a plain wing. Since the N. A. C. A. 23012 airfoil with a 0.20c N. A. C. A. 23012 external-airfoil flap has a maximum thickness equal to 10 percent of the over-all chord, it is considered directly comparable with the N. A. C. A. 23010 airfoil in that wings of these two types, having the same plan form and area, would have the same maximum thickness. The same is true of the N. A. C. A. 23021 airfoil with the N. A. C. A. 23012 external-airfoil flap in comparison with the N. A. C. A. 23018 plain airfoil.

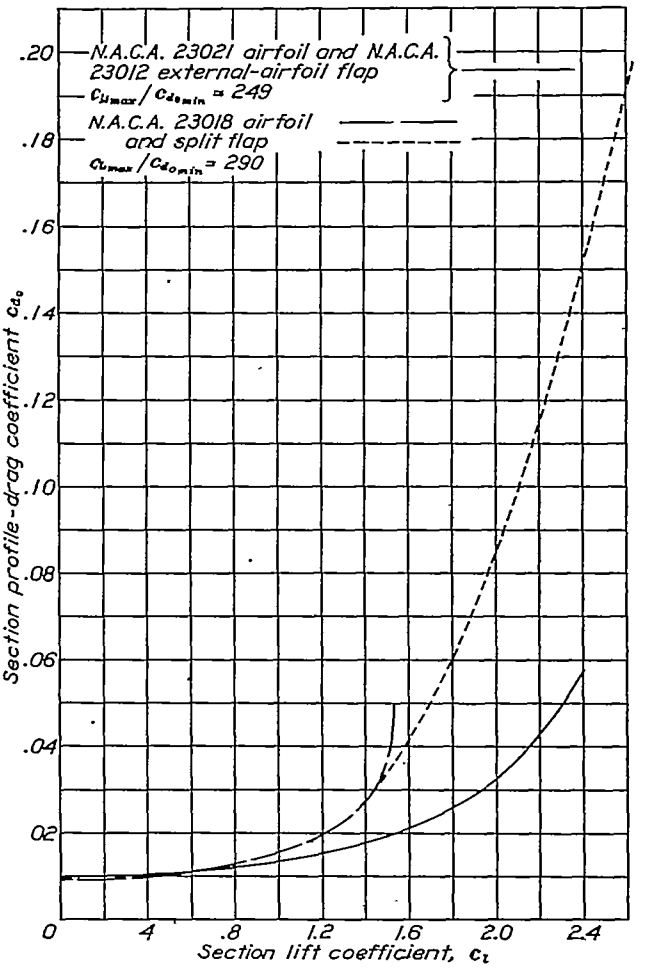

FIGURE 27.—Comparison of N. A. C. A. 23021 airfoil and 0.20c_w N. A. C. A. 23012 external-airfoil flap with N. A. C. A. 23018 airfoil and 0.20c_w split flap. Effective Reynolds Number, 8,200,000.

From the data appearing in figures 26 and 27, the advantages of the external-airfoil flap over other types of high-lift flaps in general use at present are immediately apparent. The results show that, for flight at any lift coefficient above approximately 0.7, a wing with an external-airfoil flap is superior either to the comparable plain wing or to one equipped with a split flap. Since the maximum rate of climb of most airplanes occurs at an air speed corresponding to a lift coefficient near 0.7, it is apparent that the external-airfoil flap has no adverse effect on the maximum rate of climb, provided that other factors affecting the issue, such as wing loading and span, are the same for the types of wing arrangement being compared. It is further apparent that for an airplane of a given power, weight, wing area, span, and general "cleanness" the external-airfoil flap may give appreciable improvement over the plain wing in such performance features as take-off, angle of climb, ceiling, range, endurance, and minimum rate of descent, all of which may involve flight at lift coefficients in excess of 0.7. This feature may be particularly useful in increasing the single-engine ceiling of multiengine aircraft and in permitting such airplanes to maintain flight at lower speeds, in taking off for example, than would otherwise be possible with one engine stopped.

As far as manual operation of the flap in flight is concerned, the external-airfoil flap should be considerably superior to such devices as ordinary flaps and unbalanced split flaps on account of the low values of hinge moment that can be obtained throughout the operating range. If some degree of overbalance may be tolerated in cases where the flaps are not also used as ailerons, considerably more reduction in hinge moment should be obtainable by moving the flap hinge axis farther back on the flap chord without any loss of performance characteristics. Comparison of the hinge moments obtained for either of the present flap hinge axes with the data of reference 11 indicates that this arrangement of the external-airfoil flap requires about one-third the operating moment of comparable sizes of ordinary flap throughout the normal range. This ease of operation should facilitate adjustment of the glide path in approaches to a landing and permit the use of a direct flap-operating lever on airplanes of such size that a more complicated mechanical drive would be necessary for conventional flaps. Certain other types of flap, as, for example, the Fowler or Zap, may be expected to give characteristics more nearly comparable with those of external-airfoil flaps than do the ordinary or split type. These other types, however, have extra mechanical complications in that they require some other type of motion than pure rotation, which contributes to the ease of installation and operation of external-airfoil flaps.

An undesirable feature of any trailing-edge high-lift device is the large negative pitching moment that it develops when operative. In this respect the external-airfoil flaps are slightly inferior at equal values of the maximum lift coefficient to ordinary or split flaps. In addition to the structural disadvantages involved, the problem of obtaining satisfactory balance and stability becomes more acute because of this characteristic. These features are somewhat compensated by the relatively small wake, indicated by the low drag, that occurs when the deflection of the external-airfoil flaps is less than the deflection giving the maximum lift coefficient. The reduction of tail effectiveness due to the low-speed wake, and incidentally the tendency to tail buffeting, should therefore be considerably less than with flaps that are deflected to large angles at maximum lift.

CONCLUDING REMARKS

From the data obtained in the present investigation, the external-airfoil flap in combination with an airfoil appears to be one of the most generally satisfactory high-lift devices investigated to date. The combination tested offers a relatively high value of maximum lift coefficient with low profile drag in the high-lift range. At low lift coefficients it gives very nearly as low values of profile drag as a good plain airfoil of comparable thickness. Structural and stability problems associated with the large negative pitching moments occurring at high lift coefficients may be slightly greater than in the case of ordinary and split flaps. A flight investigation of this type of device installed on a Fairchild 22 airplane, with full-span flaps arranged to operate also as ailerons, is now being conducted by the N. A. C. A.

LANGLEY MEMORIAL AERONAUTICAL LABORATORY,
NATIONAL ADVISORY COMMITTEE FOR AERONAUTICS,
LANGLEY FIELD, VA., *March 25, 1936.*

REFERENCES

1. Platt, Robert C.: Aerodynamic Characteristics of Wings with Cambered External-Airfoil Flaps, Including Lateral Control with a Full-Span Flap. T. R. No. 541, N. A. C. A., 1935.
2. Harris, Thomas A.: The 7 by 10 Foot Wind Tunnel of the National Advisory Committee for Aeronautics. T. R. No. 412, N. A. C. A., 1931.
3. Jacobs, Eastman N., and Abbott, Ira H.: The N. A. C. A. Variable-Density Wind Tunnel. T. R. No. 416, N. A. C. A., 1932.
4. Wenzinger, Carl J.: Wind-Tunnel Measurements of Air Loads on Split Flaps. T. N. No. 498, N. A. C. A., 1934.
5. Platt, Robert C.: Aerodynamic Characteristics of a Wing with Fowler Flaps Including Flap Loads, Downwash, and Calculated Effect on Take-Off. T. R. No. 534, N. A. C. A., 1935.
6. Jacobs, Eastman N., Ward, Kenneth E., and Pinkerton, Robert M.: The Characteristics of 78 Related Airfoil Sections from Tests in the Variable-Density Wind Tunnel. T. R. No. 460, N. A. C. A., 1933.
7. Jacobs, Eastman N., and Clay, William C.: Characteristics of the N. A. C. A. 23012 Airfoil from Tests in the Full-Scale and Variable-Density Tunnels. T. R. No. 530, N. A. C. A., 1935.
8. Platt, Robert C.: Turbulence Factors of N. A. C. A. Wind Tunnels as Determined by Sphere Tests. T. R. No. 558, N. A. C. A., 1936.
9. Jacobs, Eastman N., and Pinkerton, Robert M.: Tests in the Variable-Density Wind Tunnel of Related Airfoils Having the Maximum Camber Unusually Far Forward. T. R. No. 537, N. A. C. A., 1935.
10. Jacobs, Eastman N., and Pinkerton, Robert M.: Tests of N. A. C. A. Airfoils in the Variable-Density Wind Tunnel. Series 230. T. N. No. 567, N. A. C. A., 1936.
11. Wenzinger, Carl J.: Wind-Tunnel Investigation of Ordinary and Split Flaps on Airfoils of Different Profile. T. R. No. 554, N. A. C. A., 1936.

TABLE I.—AIRFOIL DATA

[See reference 9 for explanation of tabulated characteristics]

Airfoil	External airfoil flap setting, deg.	Classification				Effective R. N. millions	$C_{L_{max}}$	α_0 at $C_{L_{max}}$, deg.	Fundamental section characteristics						Derived and additional characteristics that may be used for structural design								
														a.c.			c. p. at $C_{L_{max}}$		Wing characteristics; $A=6$, round tips		Thickness			Camber, percent c
		Chord	P. D.	S. E.	$C_{L_{max}}$				α_{l_0}, deg.	a_0 per degree	$c_{l_{opt}}$	$c_{d_{0_{min}}}$	$c_{m_{a.c.}}$	Behind L. E., percent c	Above c, percent c	$\frac{C_{L_{max}}}{C_{d_{0_{min}}}}$	Computed, percent c	Actual, percent c	m_s per rad.	$C_{D_{min}}$	0.15c, percent c	0.65c, percent c	Maximum, percent c	
N. A. C. A. 23012	−3	A			A	8.21	1.62	15	−0.9	0.101	0.07	0.0069	0.009	24.0	4	235		26	4.39	0.0070	8.90	6.88	10.00	
	−3	A			D	8.16	1.04	13	.3	.086			−.013	25.2	−7			25	3.88		8.90	6.88	10.00	
	Inverted																							
	20	A			A	8.26	2.16	12	−9.0	.105	.35	.0104				208		33	4.52	.0112	8.90	6.88	10.00	
	30	A			A	8.14	2.37	12	−13.8	.102	.45	.0161				147		35	4.43	.0181	8.90	6.88	10.00	
	40	A			A	8.34	2.01	12	−15.5	.072	.26	.0329				61		33	3.36	.0342	8.90	6.88	10.00	
N. A. C. A. 23021	−3	A			A	8.20	1.52	14	−.9	.104	0	.0097	.012	23.9	6	157		26	4.49	.0097	15.58	12.03	17.50	
	−3	A			A	8.20	1.27	16	.7	.083	0	.0097	−.016	21.7	−1	131		24	3.77	.0097	15.58	12.03	17.50	
	Inverted																							
	30	A			A	8.06	2.41	11	−13.4	.108	.58	.0176				137		35	4.62	.0197	15.58	12.03	17.50	

[a] In these computations the chord length is the sum of the wing and the flap chords.